Chapter 4

The Biological Neuron

§ 1. The Diversity of Voltage-Gated Channels

Although the importance of the original Hodgkin-Huxley model can hardly be overstated, it is nonetheless a model of the giant axon of the squid. With the benefit of hindsight, today it does not seem very surprising that the whole neuron is a much more complicated object. Experimental research carried out in the 1960s eventually showed the two types of voltage-gated ion channels (VGCs) described by Hodgkin and Huxley were not the only types in existence. It was discovered that potassium channels came in many flavors. Sodium channels, too, were found to be of multiple types. Voltage-gated calcium channels were likewise discovered and rounded out the collection of major contributors to voltage-gated ionotropic current flows in the neuron cell. Even voltage-gated chloride channels have been documented [JENT].

The axon has a relatively simple task, namely the propagation of an all-or-nothing action potential. The principal signal processing tasks are carried out by the soma and dendrites of the neuron. The fast, transient Na^+ channel and the slower, persistent K^+ channel first described by Hodgkin and Huxley are adequate for the former, but inadequate to describe the latter. What is impressive, however, is the range over which the Hodgkin-Huxley modeling schema has been extended to take into account the whole neuron. Early work in extending Hodgkin-Huxley to the whole neuron appeared in 1971 in a series of papers by Connor and Stevens, leading to the Connor-Stevens model of the gastropod soma [CONN1]. Extension of the basic H-H schema is accomplished by identifying and characterizing VGC channel types and adding them in parallel to the other VGCs in the basic H-H circuit model. As Connor and Stevens remarked in a later paper,

> The strategy in this study has been to make justifiable changes in an existing system, the Hodgkin-Huxley equations, rather than pursue a competing analysis . . . We have chosen this formal and, we hope, more general approach for the following three reasons. First, we are unable at this time to justify a novel and adequate kinetic description of current carried by potassium ion in the repetitive-firing preparation and hence have tried to remain as close as possible to an existing scheme. Second, despite specific shortcomings of the Hodgkin-Huxley equations in fitting all of the available voltage clamp data from axons . . . they remain the commonly used formulation in which to cast voltage-clamp data and form the basis of the standard conceptual framework for interpreting complex electrical events in excitable cells. Third, the considerable literature on the repetitive characteristics of the equations should serve as a useful basis for criticism of this or any other analysis of repetitive activity in excitable membranes [CONN2].

Time and experience has given testimony to the soundness of the Connor-Stevens strategy and

thus far has vindicated their treatment of H-H as a modeling schema. Today we know of what has been called a "veritable zoo" of voltage-gated ion channels. Let us look at the denizens of this zoo.

§ 1.1 K^+ Channels

K^+ channels are found in all living cells and are a core feature of cellular life. In higher animals they are classified in three major groups identified by the specific "architectures" of membrane-spanning proteins [HILL4: 135]. These are named the 2TM, 4TM, and 6TM topologies, where the numerical designation identifies the number of transmembrane regions in the protein. The principal voltage-gated K^+ channels belong to the 6TM group. There are currently 24 recognized sub-families of K^+ channels, of which 16 belong to the 6TM family. Genetic analysis indicates that all 16 sub-families trace back to a common ancestral protein more than 2.4 billion years ago. Nine of the sixteen sub-families are called "delayed rectifiers" and the original K^+ channel in the Hodgkin-Huxley model belongs to this group.

At least two sub-families in the 6TM group, the "mslo" and "SK1" sub-families, are modulated by concentration levels of cytoplasmic free Ca^{2+}. Some of these (the "BK" group of the mslo sub-family) are also voltage-dependent. Their single-channel conductances, g_p, range from as low as 4 pS to as high as 250 pS [HILL4: 144].

The seven sub-families in the 2TM group are called "inward rectifiers." These have the interesting property that they *stop conducting* under membrane depolarization and *increase conduction* under hyperpolarization. This is the precise opposite of behavior we saw for the K^+ VGC in the squid axon. The membrane voltage at which they open and begin conducting is a function of the extra-cellular K^+ concentration, generally increasing (getting closer to 0 volts) as $[K^+]_o$ increases. They are also characterized by at least *two* time constants, one very fast (less than 1 ms) and the other ranging from milliseconds to 0.5 seconds, depending on the particular channel protein. Because glial cells are thought to regulate the levels of $[K^+]_o$ here is one speculative mechanism by which it might be possible for glia to participate in biological signal processing. Some (the Kir6 sub-family, also called K_{ATP}) open and hyperpolarize the cell when the level of ATP (adenosine triphosphate, a molecule responsible for powering the metabolism of a cell) falls low. One could say this channel "shuts down" neurons that are low on energy. Some K^+ channels, belonging to the Kir8 sub-family, are regulated by metabotropic signaling processes and can be opened in response to hormone or neuromodulator signaling.

Exploration of the 4TM family is not yet very far along. It has currently not been divided into sub-families, although future research is expected by many to reveal a rich sub-family tree similar

to those of the other two families. The 4TM channels that have been studied have not shown any strong voltage dependency and their presently known role seems to be that of "leakage" channels that help determine the membrane resting potential. Some are known to be closed by metabotropic signaling processes, and these would appear to constitute another mechanism by which the activity of a neuron can be modulated.

The various K^+ channels play significant roles in modifying how a basic H-H-like circuit responds to different stimuli. For example, McCormick and Huguenard identified four distinct types of K^+ channels, one of which is a leakage channel, present in single thalamocortical relay neurons in the dorsal lateral geniculate nucleus (LGN)[1] of rodents and cats [McCO]. McCormick has described some of the effects these channels have on cell signaling properties in [McCO1]. The list of known distinct types of K^+ channels is long and impressive. We will not do an in-depth review of the specific channel types in this book. Extensive reviews are provided by Rudy [RUDY] and by Storm [STOR].

§ 1.2 Na^+ Channels

Na^+ VGCs are much less diverse than the K^+ channels and belong to a different genetic "family tree." They descend from a 24TM protein "architecture." Na^+ channels are classified into 9 different channel types. Interestingly, the Na^+ channels appear to have branched off from one line of Ca^{2+} channel proteins about 800 million years ago [HILL4: 721]. They are classified according to amino acid sequences and bear the rather simple names $Na_v1.1$ through $Na_v1.9$. The closer numerically the last digit is to another channel, the more similar are their amino acid sequences.

Functionally, Na^+ channels are divided into two groups, typically called $Na_{(fast)}$ and $Na_{(slow)}$ but also called Na_t (for "transient") and Na_p (for "persistent"). The former is the class described by the H-H model (that is, it is an "inactivating" channel). In the case of the latter, it is often not altogether clear if the channel is non-inactivating or if it is merely an inactivating channel with a very large inactivation time constant. Functionally, this latter fine point seems to make no known important difference insofar as biological signal processing is concerned since if it is "slowly inactivating" rather than non-inactivating, the neuron's signaling response seems the same in either case. That is one reason for calling them "persistent" rather than inactivating vs. non-inactivating.

Transient ("fast") Na^+ channels typically have an activation threshold around about –50 mV. They are the VGCs responsible for generation of the action potential. Persistent channels

[1] The LGN is part of the thalamus, which is the main "switchboard" for sensory information en route to the neocortex from the peripheral nervous system.

typically have an activation threshold of around –65 mV, and thus some number of them may be open already at the neuron's resting potential [JoWu: 208]. If these really are non-inactivating (as opposed to extremely slowly inactivating), they would constitute a form of "leakage" channel for the neuron at rest if the neuron's resting potential is $V_r > -65$ mV. Nonetheless, they are still VGCs. McCormick and Huguenard [McCO] described their persistent Na channel using an expression of the form $I_{Nap} = g_{max} \cdot (V_m - E_{Na}) \cdot m$.[2] Unlike the H-H model, m was given as a direct function of the membrane voltage and not from a differential equation describing a rate process. Thus their m does not have an interpretation in terms of gating kinetics. Rather, it is obtained based on experimental findings by French et al. [FREN].

French and his colleagues were able to demonstrate the existence of a voltage-activated and persistent Na^+ channel in rat hippocampus. The French model is a curve-fit to measured data, and they were able to fit their results to a function of the form

$$G_{Na} = \frac{g_{max}}{1 + \exp\left[\left(V_{50} - V_m\right)/k\right]} \quad . \tag{4.1}$$

An equation of the form of (4.1) is called a ***Boltzmann equation***, named after the Boltzmann distribution function in classical statistical mechanics. Here V_{50} is the membrane voltage at which 50% of the peak value of conductance occurs, V_m is the membrane voltage, and k is a constant. They reported the best fit to their experimental data for $V_{50} = -50$ mV and $k = 9$ mV. Their g_{max} averaged 7.8 ± 1.1 nS for the whole neuron and 4.4 ± 1.6 nS for dissociated cell bodies (neurons that had their dendrites removed, leaving only the soma and some dendrite "stubs"). This pair of findings led them to conclude the majority of Na_p channels were located on or near the soma. By estimating the cell's surface area from measurements of its capacitance and assuming 1.0 μF/cm^2, they estimated the specific g_{max} at 1.7 ± 0.6 pS/μm^2.[3] This compares to a measured specific maximum conductance for the transient Na^+ channels of 113 ± 11.6 pS/μm^2. Thus either the g_p for the persistent channel is some sixty times smaller than that of the transient channel pore (which seems unlikely), or the pore density is some sixty times less, or some combination of lower maximum conductance and lower density characterizes the persistent channel.

The nature of the experimental technique used by French et al. did not permit them to characterize the gating kinetics of the persistent Na^+ channel because these kinetics were masked by the large-amplitude action potentials the neurons produced in response to stimulus. All that

[2] A negative current in their model denotes current flow *into* the cytoplasm. This has become a more or less standard convention among physiologists today.
[3] A "specific" g_{max} is defined as g_{max} per unit area.

can be confidently concluded from their experiment is that the activation gate of the persistent channel opens no more slowly than the inactivation gate of the transient channel closes. When g_{max} in (4.1) is set to 1 we obtain the *m* variable used by McCormick and Huguenard. It still ranges from 0 to 1, and can still be interpreted in terms of the fraction of available channels that are open. It does not, however, have an associated time constant. This does not mean the physiological channel has no time constant; it merely means we do not know what it is.

It is not inappropriate to mention here that some channels not belonging to the Na^+ family also conduct Na^+ currents along with K^+ currents. These are usually vaguely referred to as "cation channels." In addition, some of the hyperpolarized K^+ slow inward-rectifier channels also conduct some amount of Na^+. As remarked upon in chapter 1, the "leakage circuit" part of a H-H-like circuit model can hide some rather interesting physiology.

§ 1.3 Ca^{2+} Channels

Calcium ions are one of the most potent metabotropic chemical "messengers" known. Free Ca^{2+} ions in the cytoplasm are responsible for a vast range of effects, including long-lasting changes currently thought to be the biological basis for learning and memory. Free Ca^{2+} levels within the neuron are kept very low, on the order of 50 to 100 nM, by the action of various internal cell structures that capture and "warehouse" calcium, and by the action of calcium pumps. In most neurons a structure called the endoplasmic reticulum (ER) serves as the primary "warehouse" for stored calcium. A typical $[Ca^{2+}]_o$ concentration is on the order of about 2.0 mM and so a Nernst potential for Ca^{2+} at 290 kelvin would range from +124 to + 132 mV.

There are two major divisions of Ca^{2+} channels, called the high-voltage activated (HVA) and low-voltage activated (LVA) Ca channels. The HVA group is further divided into two branches, called the L branch and the "second branch." The L branch of the HVA group contains four sub-families of channels (called $Ca_v1.1$ through 1.4). These channels are slow, persistent ion channels. Their activation threshold is about –30 mV. Although called "persistent" channels, they do have an inactivation range (about –60 to –10 mV) but their inactivation time constants are greater than 500 ms [HILL4: 117]. They deactivate rapidly in the range from –80 to –50 mV and have a single channel conductance g_p of about 25 pS.

The second HVA branch contains three sub-families (called $Ca_v2.1$ through 2.3, and also often called the P/Q, N, and R channels). These are transient channels with an activation threshold of about –20 mV. Their inactivation range is from –120 to –30 mV with inactivation time constants in the range from 50 to 80 ms. They deactivate slowly in the range from –80 to –50 mV and have a single channel conductance g_p of about 13 pS [HILL4: 117]. Both branches of HVA channels

are found in presynaptic terminals, and they are responsible for triggering neurotransmitter exocytosis in response to action potentials. Their activation thresholds account for the value of Ω stated in chapter 3 for the model of synaptic LGC conductance. HVA channels have also been found outside the presynaptic terminal, although their role here is not certain (owing to their high activation threshold).

The LVA channel branch contains three sub-families, denoted $Ca_v3.1$ through 3.3. These are also often called T-channels. As the name implies, their activation threshold is low, about –70 mV. They are transient channels with an inactivation range from –100 to –60 mV. Thus, for the typical neuron at its resting potential these channels are inactivated. Hyperpolarization rapidly deactivates them, and then their low activation threshold causes them to re-open briefly. One interesting consequence of this is a phenomenon called ***post-inhibitory rebound***. In some neurons, inhibitory synaptic signals are followed, after cessation of inhibition, by the generation of a single action potential spike. This phenomenon is thought to be due to the T-channels re-activating after deep hyperpolarization. A typical value for g_p in these channels is about 8 pS [HILL4: 117].

Genetic analysis suggests both branches of Ca^{2+} channels stem from a common ancestral protein, probably about 1.8 billion years ago. In turn, this common ancestor is thought to have descended from an earlier 6TM ancestor more than 2.4 billion years ago. It is possible that this common ancestor might also have been the ancestor of the 6TM line of K^+ VGCs [HILL4: 721].

§ 2. Extending and Augmenting the Hodgkin-Huxley Model

The presence of so many different kinds of VGCs, each with differing gating kinetics and voltage dependencies, makes it necessary to extend the basic Hodgkin-Huxley model. Furthermore, the presence of Ca^{2+} channels poses an additional consideration. While the battery potentials E_{Na} and E_K are not changed significantly by their respective ion flows (because the ion concentrations in the cytoplasm and extracellular region do not change by a large enough amount to significantly affect the Nernst potential), the situation is quite different in the case of calcium. The normal concentration of cytoplasmic free Ca^{2+} for the cell at rest is quite low, and so the influx of Ca^{2+} via calcium VGCs is sufficient to register an effect on E_{Ca}.

Physiologists usually account for this effect by replacing the relatively simple expressions for ion current flow we have been using with the Goldman-Hodgkin-Katz current equation (which will be presented later). Furthermore, the calcium-dependent family of K^+ channels also has a conductance that explicitly depends of the concentration of cytoplasmic free calcium. In order to properly model both effects, the cytoplasmic concentration of free Ca^{2+}, which we will denote

using the symbol $[Ca]_f$, must be explicitly accounted for. Thus, $[Ca]_f$ must be made an additional state variable in the model of the neuron. This is called ***augmenting*** the Hodgkin-Huxley model.

§ 2.1 Extending the Ion Channel Model

We will begin with the method for extending a VGC model for one particular ion, say K^+ or Na^+, to account for the variety of membrane-spanning proteins that conduct the overall ion current. It has previously been noted the total conductance of a channel is the sum of the conductances of the individual open pores. If these pores have different gating kinetics and different voltage dependencies, we must divide the total channel conductance, $G(t)$, into a sum of conductances for the different channel types. For example, suppose we have two distinct types of K^+ channel proteins. Since each would have the same E_K potential, we would write the total channel conductance as the sum of two terms, i.e. $G(t) = G_1(t) + G_2(t)$. This is illustrated by Figure 4.1 below. The circuit at the left in this figure is called a Thévenin equivalent of the circuit on the right. This equivalence method can be extended to include as many different species of ion channels for a particular ion as necessary. For example, McCormick's and Huguenard's thalamo-cortical relay neuron model [McCO], [HUGU] contains two types of Na channels, four types of K channels, two Ca channels, a sodium leakage channel, and a potassium leakage channel for a total of ten specific channels.

§ 2.2 Calcium Channels

Levels of free calcium in the cytoplasm are always extremely low. Typical concentrations of free Ca^{2+} in the cytoplasm are in the range of 50 to 100 nM. (1 M = 1 mole per liter). This is six orders of magnitude less than the concentration level of free Na^+ in the cytoplasm. This low level of free Ca^{2+} is caused and maintained by physiochemical processes in the cell for transporting and

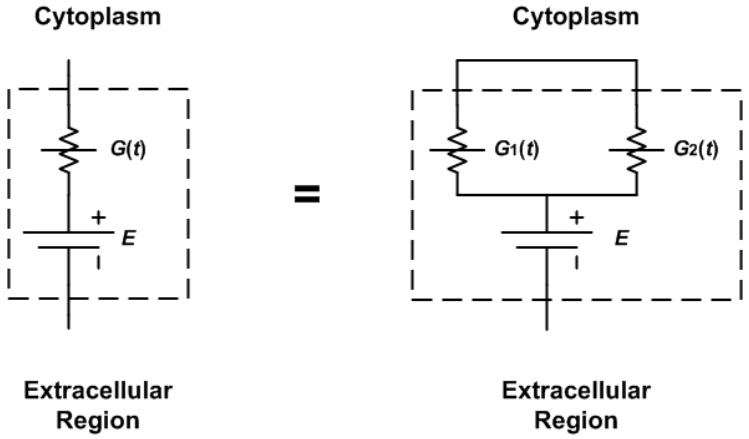

Figure 4.1: Extending an ion channel into two components.

storing calcium and for returning Ca^{2+} to the extracellular region [HILL4: 269-306]. The immediate consequence of this is that it is rather meaningless to try to assign a Nernst potential for calcium channels. Even if the membrane potential V_m becomes positive, either due to action potential generation or because of voltage clamp measurements, the cytoplasm contains so few free Ca^{2+} ions relative to the extracellular region that no outward flow of calcium current results. Physically, a Nernst potential is the representation of a condition of thermodynamic equilibrium, but calcium channel current flow is an inherently non-equilibrium thermodynamics phenomenon.

For this reason, and for the practical reason that attempts to describe Ca^{2+} currents in the same way Na^+ and K^+ are described do not work, models of calcium VGCs are based on another theoretical approach, called ***constant-field theory***, originally developed in 1939 by Nevill Mott for describing electron conduction in a copper/copper oxide rectifier. D.E. Goldman introduced the method to biology in 1943 [GOLD], and the theory was further polished up and developed by Hodgkin and Katz in 1949 [HODG7]. The result is the Goldman-Hodgkin-Katz (GHK) current equation.

The GHK current equation[4] models the current density (current per unit area) flowing through a permeable membrane as a function of membrane voltage and ion concentrations. We will only consider Ca^{2+} currents here, but the GHK current equation applies equally well to other kinds of ion flux. ***Flux density*** is defined as the number of particles flowing per unit area of cross section per unit time for a group of particles moving in an organized manner. (The integral of flux density taken across the entire surface area is called the particle ***flux***). When the number of particles is expressed in moles (1 mol = Avogadro's number of particles), the flux density is called the ***molar flux density*** (which is usually expressed in units of $mol/cm^2 \cdot s$). The ***permeability constant*** P of the membrane (often just called its "permeability") is defined to be the ratio of the molar flux density to the difference in ion concentrations on the two sides of the membrane. When the concentrations are expressed in units of moles per cm^3 (moles per milliliter) and the molar flux density is expressed as before, the permeability constant has the units of cm/s. Formally, P is merely a mathematical quantity meant to convey in some sense how "easy" or "hard" it is for an ion to penetrate through the membrane. At our present state of knowledge we cannot derive P from more fundamental considerations, and its quantity is experimentally determined. In making this determination it is not unusual for the measured quantity to actually be the product of this mathematical permeability constant and the surface area of the cell, $p = PA$. P is then determined by dividing out the surface area.

[4] There is also a GHK voltage equation. It is often used by theoretical biologists, but we will have little need of it in this text.

Armed with these ideas, the GHK current equation is derived from the ***Nernst-Planck*** equation for electrodiffusion, which describes ion motion [HILL4: 312-319]. The final result can be written[5] as

$$i_{\text{GHK}} = s \cdot P \frac{zF}{V_{th}} \frac{\left[Ca^{2+}\right]_{\text{i}} \cdot \exp\left(V_m / V_{th}\right) - \left[Ca^{2+}\right]_{\text{o}}}{\exp\left(V_m / V_{th}\right) - 1} \cdot V_m \tag{4.2}$$

where $V_{th} = kT/ze$ is called the ***thermal equivalent voltage***, V_m is the membrane potential (relative to the extracellular region), $F = 9.6485 \cdot 10^4$ coulomb/mole is Faraday's constant, $z = 2$ is the valence of Ca^{2+}, and i_{GHK} is the current density. s is a scale factor that depends on the units used to express the concentrations and the permeability. When P is in cm/s and the concentrations are expressed in moles per milliliter, $s = 1$ and i_{GHK} has units of amperes/cm^2. If the concentrations are expressed in nM (10^{-9} moles/liter) and s is set to 1000, then i_{GHK} is in nA/cm^2.

To obtain the Ca^{2+} channel currents for the whole cell, we factor in the gating dynamics of the voltage-dependent calcium pores and either multiply i_{GHK} by the surface area A (in cm^2) or, equivalently, replace P by $p = PA$ in (4.2). This gives us

$$I_{Ca}\left(V_m\right) = m_{Ca}^{j} h_{Ca}^{q} s \cdot p_{\max} \frac{zF}{V_{th}} \frac{\left[Ca^{2+}\right]_{\text{i}} \cdot \exp\left(V_m / V_{th}\right) - \left[Ca^{2+}\right]_{\text{o}}}{\exp\left(V_m / V_{th}\right) - 1} \cdot V_m \tag{4.3}$$

where m_{Ca} and h_{Ca} are the activation and inactivation gate factors. A typical empirical value for L-type Ca^{2+} and T-type Ca^{2+} channels is $j = 2$. $p_{\max}$ is called the maximum permeability factor and has units of cm^3/s. If the cell's internal mechanisms for clearing out free Ca^{2+} (called "calcium buffering") are efficient, then $q = 0$ and the channel is non-inactivating[6]. As an example of the activation gate kinetics, McCormick and Huguenard used the following expressions for the high-voltage L-type channel in thalamocortical relay neurons:

$$\begin{aligned} m_{Ca} &= \frac{\alpha}{\alpha + \beta} \\ \alpha &= \frac{1.6}{1 + \exp\left(-0.072 \cdot \left(V_m - 5.0\right)\right)} \\ \beta &= \frac{0.02 \cdot \left(V_m - 1.31\right)}{\exp\left[\left(V_m - 1.31\right)/5.36\right] - 1} \end{aligned} \tag{4.4}$$

with V_m expressed in mV. As always, these three quantities are dimensionless.

[5] Biologists and chemists are accustomed to seeing the GHK current equation in a different form from this. To obtain this expression we make use of the identity $R/F = k/e$, where k is the Boltzmann constant.

[6] It is known that for calcium channels h is a function of $[Ca^{2+}]_{\text{i}}$. If something interferes with the calcium buffering mechanisms, allowing a large rise in free cytoplasmic calcium, the channel is inactivating.

Biologists usually do not express the calcium channel in terms of a conductance, although by noting that (4.3) is in the form of something times the membrane voltage, we are perfectly free to regard this expression as a conductance, i.e.,

$$G_{\mathrm{GHK}}\left(V_m, Ca^{2+}\right) \stackrel{\Delta}{=} m_{Ca}^{j} h_{Ca}^{q} \cdot s \cdot p_{\max} \cdot \frac{zF}{V_{th}} \cdot \frac{\left[Ca^{2+}\right]_{\mathrm{i}} \cdot \exp\left(V_m / V_{th}\right) - \left[Ca^{2+}\right]_{\mathrm{o}}}{\exp\left(V_m / V_{th}\right) - 1} . \qquad (4.5)$$

Doing this is equivalent to saying the calcium battery potential is $E_{Ca} = 0$. This G_{GHK} is, however, a rather exotic conductance. First we note that it is ***calcium dependent*** as well as voltage dependent. The extracellular calcium concentration can be regarded as constant (typically with a value of about 2 mM), but the free cytoplasmic calcium concentration is not. Therefore, in simulations this expression *must be augmented* by a model component describing the concentration of free $[Ca^{2+}]_{\mathrm{i}}$. Second, note that for $V_m = 0$, the denominator of (4.5) goes to zero, meaning G_{GHK} is infinite (like a "short circuit"). However, (4.3) remains finite because

$$\lim_{V_m \to 0} \frac{V_m}{\exp\left(V_m / V_{th}\right) - 1} \to V_{th}$$

and so I_{Ca} remains finite and well-defined. For $V_m < 0$, G_{GHK} is positive (because the extracellular calcium concentration is so much larger than the free cytoplasmic calcium concentration). But for $V_m > 0$ there is a range of membrane voltages for which G_{GHK} is *negative*. Electrical engineers are used to dealing with negative resistances and negative conductances – they are a commonplace occurrence in feedback circuits containing active gain elements such as transistors – but the occurrence of negative conductance in a biological model severely clouds the issue of making any sort of interpretation of the *physical* significance of G_{GHK}. Certainly we lose the comfortable mental picture of channel conductance as the simple conductance of a pore in a membrane. What one should bear in mind is that constant-field theory is at best an approximate theory and makes a number of simplifying assumptions that do not stand up under close physiological scrutiny. As Bertil Hill has remarked,

> The GHK theory is a superb tool for reporting results, but is less useful as a guide to the physical structure of channels. Two quite different concepts of solubility-diffusion theory – the partition coefficient and the mobility – are blended into one permeability parameter. The channel is assumed to be homogeneous. The ions are assumed not to interact either physically or electrostatically. But these assumptions are wrong, so the predictions cannot be right in detail. Indeed, the deviations from GHK theory . . . have stimulated the major advances since 1970 [HILL4: 449].

If we bear this in mind and understand that G_{GHK} is a *mathematical* creature, we can go ahead and use (4.5), understanding we are not to read into it things that are simply not there.

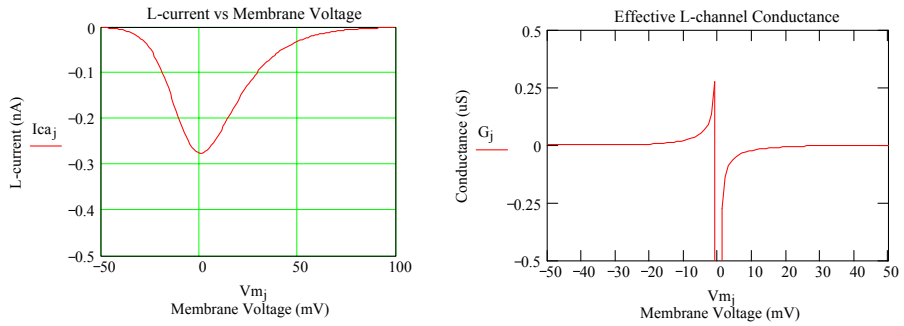

Figure 4.2: I_{Ca} and G_{GHK} steady-state curves with $[Ca^{2+}]_i$ held constant for an L-type Ca^{2+} channel.

Although there is no particular physiological value to doing so, it is instructive to plot (4.3) and (4.5) as functions of membrane voltage with $[Ca^{2+}]_i$ held constant and with $m = m_\infty$. This is done in Figure 4.2 using $p_{max} = 1$ cm^3/s, $[Ca^{2+}]_i = 50$ nM, $[Ca^{2+}]_o = 2$ mM, $T = 297$ kelvin, $j = 2$, and $q = 0$. The McCormick-Huguenard expressions (4.4) were used to calculate m. (4.3) was scaled to give I_{Ca} in nA, and V_m and V_{th} are in mV. G_{GHK} is in μS.

Our first observation is that I_{Ca} is negative (denoting current flowing into the cytoplasm) for all values of V_m. The peak occurs just slightly above $V_m = 0$, and the half-maximum current first occurs at around $V_m = –15$ mV. This illustrates why the L-type Ca^{2+} channel is called a high-voltage-activated (HVA) channel. G_{GHK} is positive for all $V_m < 0$. It has a singularity at $V_m = 0$ and is negative throughout the range of $V_m > 0$ shown in the plot. These plots are instructive for the purpose of gaining a qualitative "picture" of the properties of the calcium channel, although the artificial constraint of keeping the calcium concentrations constant prevents us from making serious quantitative judgments of how the channel will behave in simulation. Their usefulness is akin to the steady-state activation variable and time constant plots in chapter 3 for the Hodgkin-Huxley model. Note, too, the singularity at $V_m = 0$ is a feature of G_{GHK} that is independent of calcium concentrations for any physiological numerical values for these concentrations.

LVA calcium channels are also usually modeled using the GHK current equation method, although there are exceptions to this in the modeling literature. The two principal differences between LVA curves and HVA curves are these: (1) the activation voltage for the LVA channel shifts dramatically to the left, from about –15 mV to around –40 mV; (2) the LVA channel is a rapidly inactivating channel ($q = 1$) and requires Hodgkin-Huxley-like expressions for the voltage-dependent inactivation factor h. This is often in the form of a Boltzmann equation (V_{50} on the order of about –80 mV, the Boltzmann equation k factor on the order of about –4 mV). It is a peculiarity of the LVA T-type channel that its time constant function is often biphasic, i.e, the curve fit equation for $V_m < V_{50}$ and that for $V_m > V_{50}$ are often different. An example of this is

provided by [HUGU].

§ 2.3 The Linvill Modeling Schema

Models of cytoplasmic Ca^{2+} concentration in neurons are usually fairly simple, direct, and to the point. Nonetheless, there is something to be said in favor of having a general and versatile modeling schema for particle accumulation, transport, chemical reaction, and storage in the cell. A general schema is an aid for transforming qualitative models into quantitative ones and for developing relationships descriptive of more complex physiological processes. After all, if the Hodgkin-Huxley schema is useful in part because it provides a guide for dealing with the complexities of VGC and LGC signaling, is it not also likely that a similar schema might prove useful for dealing with cellular biochemical signaling processes?

In this text we resurrect and adapt to our purposes a modeling schema originally developed in 1958 by John G. Linvill [LINV: 17-48] and extended to application in neuroscience by his former student, Wells, in 2007. The Linvill model was developed to represent carrier transport, storage, and generation-recombination phenomena in semiconductors in terms of carrier densities and current flows. The model had never previously been applied to biological signaling processing models. After all, the neuron is not a transistor or a diode. Nonetheless, with only a few minor adaptations of the Linvill model, we can apply its as a schema for representing ion flux and concentration in the cell. This section introduces the basic modeling elements and their mathematical description. The next section applies it to the relatively simple task of modeling cytoplasmic free Ca^{2+} concentration.

The Linvill modeling schema allows us to represent the model as a network of elements, each of which is characterized by a specific ***element law***. Figure 4.3 illustrates the five basic Linvill network elements.[7] Ion or molecule concentration is denoted by the symbol v. Ion or molecule flux is denoted by the symbol ϕ. Flux is positive in the direction denoted by the arrows.

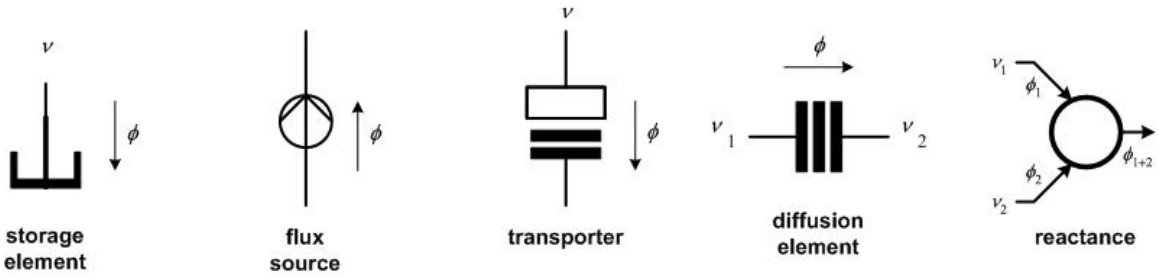

Figure 4.3: The five basic network elements of the Linvill modeling schema.

[7] The notations and variables used here are modified from Linvill's original form. Linvill was concerned with modeling charge densities and currents, whereas we have broader and more diverse needs.

Particle (ion or molecule) motion in space is formally describable in terms of partial differential equations with boundary conditions. While such a description is mathematically rigorous and precise, it is also rather cumbersome and computationally difficult to deal with in all but the simplest cases of physical geometries. This issue is often overcome in the various sciences through the introduction of the ***lumped element*** approximation. For example, electric and magnetic phenomena are rigorously described by Maxwell's equations, a set of partial differential equations. ***Circuit theory*** is the lumped element approximation of these equations, applicable when electromagnetic radiation (a consequence of Maxwell's equations) is not an important factor. (Neglect of radiation effects is called the ***quasi-static approximation***). Similarly, the Linvill model is a lumped element approximation to the partial differential equation description of particle transport, storage, and accumulation.

The storage element ("**storance**") represents the accumulation of particles in a region due to influx from some other location or source. Its v-ϕ relationship is based on the mathematical form of the divergence theorem which, in nontechnical language, merely states, "What goes in must come out or else remain inside." The element law merely states that the net influx of particles into the storage element is proportional to the time rate of change of concentration,

$$C\frac{dv}{dt} \stackrel{\Delta}{=} C\dot{v} = \phi \tag{4.6}$$

Dimensional analysis shows C has units of volume. C reflects the fact that a region of greater volume builds up particle concentration less rapidly than a region of smaller volume for the same amount of flux. We may at once note the similarity between (4.6) and the element law for a capacitor in circuit theory. ϕ is analogous to electric current and v is analogous to voltage. There are, however, limits to this electric circuit analogy. The accumulation of v in a storage element does not induce the accumulation of some other particle elsewhere (no equivalent to charge on one plate of a capacitor inducing the opposite charge on the other plate), and there is nothing analogous to the "displacement current" through a capacitor which is a consequence of the Maxwell equations. Likewise, there is no "Kirchhoff's voltage law" for this network. Particle flux is not required to flow in a closed circuit path (hence the model is a "network" model rather than a "circuit" model). Particle *conservation*, however, *is* required for the first four network elements because only the **reactance** element represents a chemical reaction, e.g. a + b $\rightarrow$ c.

The flux source element represents influx/efflux from some exterior source. Our most common use for this element will be to convert electric currents obtained from the H-H model to particle flux. The current I due to a flux ϕ of particles with valence z is simply $I = ze\phi$ when ϕ is

expressed in particles per second. It is more convenient, however, to express flux in units such as moles/second. In this case we would write $I = zF\phi$, where F is Faraday's constant. (If we had a current *density* – amperes per unit area – we would replace flux by flux density). Letting $\beta = 1/zF$ we obtain the element law as $\phi = \beta \cdot I$ with I in amperes and β in moles/coulomb. For $z = 1$, β is numerically equal to $10.3643 \cdot 10^{-6}$ moles/coulomb; it is one-half this value if $z = 2$. Note that the sign of the valence is irrelevant to flux (since this is merely the sign of the electric charge carried). Therefore if one is modeling the flux of a negative-valence particle, the absolute value of z would be used.

The transporter symbol is our generalization of an element Linvill called a "**combinance**" [LINV: 25]. In his original model this element was used to model charge generation and recombination in semiconductors. That is a process by which *bound* charge is converted to *free* charge and vice versa. The analog to this within the cell (not including chemical reactions that produce new compounds) are the processes by which free particles are introduced or removed by various transport processes, such as the transport process by which free Ca^{2+} is removed from the cytoplasm and stored in the endoplasmic reticulum [HILL4: 269-273]. In effect, these are pumping processes in which the average flux is determined by the amount of particle transport per cycle of the pump and the concentration of the particle being transported. Thus, the simplest form of an element law for the transporter is the relationship

$$\phi = \rho \cdot \nu \tag{4.7}$$

where ρ is an empirically-determined transport parameter with units of volume/second. Note that this expression is unidirectional. The concentration variable in (4.7) is placed at the "boxed" end of the network element, and whatever the concentration may be at the other terminal is irrelevant. The transporter does not represent a passive diffusion process. That dynamic is modeled by the fourth network element.

The diffusion element ("**diffusance**") represents particle flux due to concentration differences. Flux is positive in the direction from higher concentration to lower concentration. In its simplest form, the diffuser element law is merely

$$\phi = D \cdot (\nu_1 - \nu_2) \tag{4.8}$$

where D is an empirically-determined parameter with units of volume/second.

If C, ρ, and D are represented by simple constants we have a *linear* model of transport and storage. Making these variables functions of ν, and possibly other variables, produces a nonlinear model. At our present state of knowledge of neural physiology no nonlinear model of the

neuron's internal processes is in widespread use and, consequently, most neuron modeling work has used a linear model of the cytoplasmic Ca^{2+} transport and storage processes.

Using the first four elements we can construct network models of arbitrary complexity to represent various transport and storage processes excepting those involving chemical reactions (for which we need to represent what happens to the reaction compounds afterward). Chemical reactions are modeled by the **reactance** element, which is discussed at the end of this chapter. If it happens to be the case where we do not care what happens later to these reaction products, a transporter element (called a **reactor** in this case) combined with a storage element can suffice for representing the introduction or the removal of free particles. The next section illustrates the application of this modeling schema to Ca^{2+} augmentation of the basic H-H model.

§ 2.4 Simple Models of Ca^{2+} Processes in the Neuron

The simplest and most common model of Ca^{2+} buffering in the neuron represents the gross influx of Ca^{2+} from calcium channels and the removal of free Ca^{2+} from the cytoplasm by a transport process. Figure 4.4 illustrates the model network. The endoplasmic reticulum is regarded as having infinite volume and so the time rate of change of $[Ca^{2+}]$ at this node is zero. I_{Ca} is obtained from the electrical model of the neuron and its numerical value is negative or zero. Thus, the network of Figure 4.4 receives an influx of Ca^{2+} into node v. Summing the effluxes from this node, we obtain the dynamical equation

$$C\frac{dv}{dt} = -\rho \cdot v - \beta \cdot I_{Ca}(t) \ . \tag{4.9}$$

We convert (4.9) to difference equation form by the same method used previously.

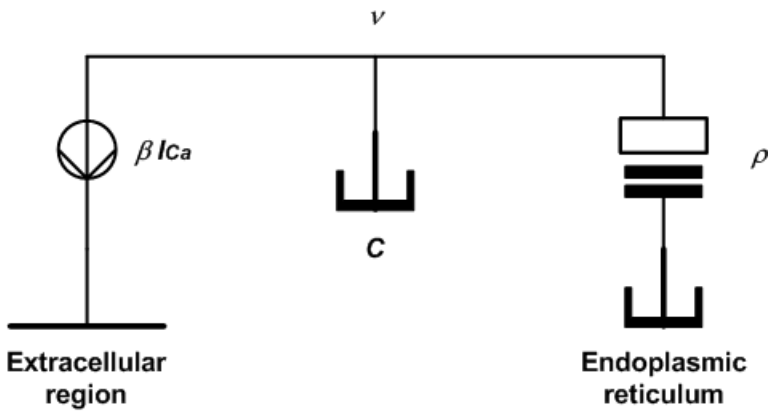

Figure 4.4: Simple model of free Ca^{2+} buffering. I_{Ca} is obtained from the electrical model of the neuron. Because its numerical value is negative, the Ca network receives a Ca^{2+} influx.

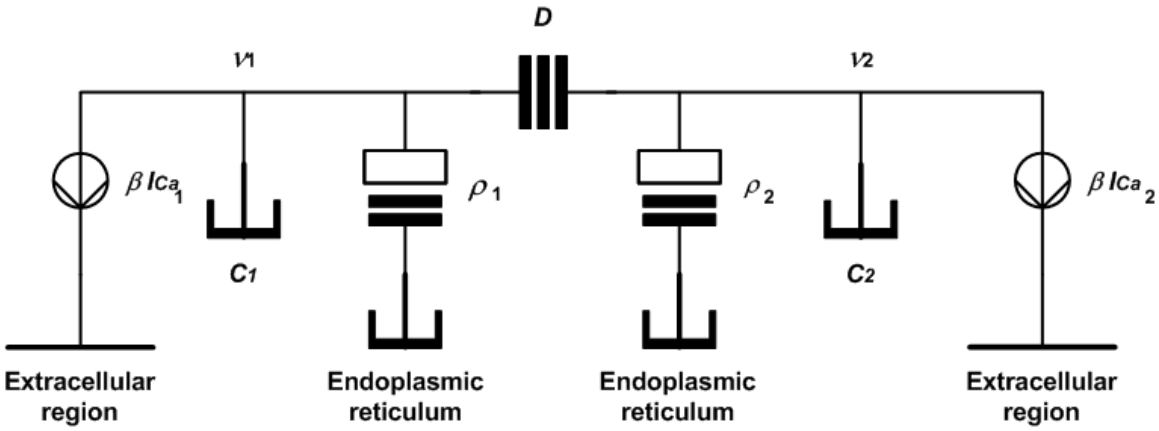

Figure 4.5: Two-compartment model of a Ca^{2+} network.

Most calcium buffering models incorporate a constraint that the minimum level of $[Ca^{2+}]_i$ is not allowed to fall below some minimum value $[Ca^{2+}]_{min}$. This is easily incorporated into the network of Figure 4.4 by adding a phenomenological "calcium leakage flux" in parallel with the calcium flux obtained from the electrical model. Setting the derivative in (4.9) to zero, we obtain for this leakage flux the numerical value $\beta \cdot I_{leak} = -\rho \cdot [Ca^{2+}]_{min}$. The direction of the arrow for this flux source is the same as that of the source shown in Figure 4.4.

McCormick and Huguenard [McCO] argued that the literature on neuron physiology suggested HVA calcium channels, $I_{Ca(L)}$, and LVA T-current channels, $I_{Ca(T)}$, are probably located in different regions of the neuron. They used this argument to justify making their Ca^{2+}-dependent K^+ VGC element depend on the contribution to $[Ca^{2+}]$ from the L-current only. In their model they kept track of the individual contributions from $I_{Ca(L)}$ and $I_{Ca(T)}$ while still letting their GHK current model depend on the sum of the two components. In effect, their model is something like a two-compartment model of the calcium network, although not entirely rigorous in its formulation. A more formal representation of two-compartment modeling is illustrated in Figure 4.5. The schema is easily extended for representing any number of calcium compartments.

Summing the effluxes from each node and rearranging terms we obtain a system of two differential equations,

$$\begin{bmatrix} dv_1/dt \\ dv_2/dt \end{bmatrix} = \begin{bmatrix} -(\rho_1 + D)/C_1 & D/C_1 \\ D/C_2 & -(\rho_2 + D)/C_2 \end{bmatrix} \begin{bmatrix} v_1 \\ v_2 \end{bmatrix} + \begin{bmatrix} -\beta_1/C_1 & 0 \\ 0 & -\beta_2/C_2 \end{bmatrix} \begin{bmatrix} I_{Ca_1} \\ I_{Ca_2} \end{bmatrix}. \qquad (4.10)$$

Using Euler's method, the corresponding difference equation representation is

$$\begin{bmatrix} v_1(t+\Delta t) \\ v_2(t+\Delta t) \end{bmatrix} = \begin{bmatrix} 1-\Delta t \cdot (\rho_1 + D)/C_1 & \Delta t \cdot D/C_1 \\ \Delta t \cdot D/C_2 & 1-\Delta t \cdot (\rho_2 + D)/C_2 \end{bmatrix} \begin{bmatrix} v_1(t) \\ v_2(t) \end{bmatrix} + \begin{bmatrix} -\Delta t \cdot \beta_1/C_1 & 0 \\ 0 & -\Delta t \cdot \beta_2/C_2 \end{bmatrix} \begin{bmatrix} I_{Ca_1}(t) \\ I_{Ca_2}(t) \end{bmatrix}.$$

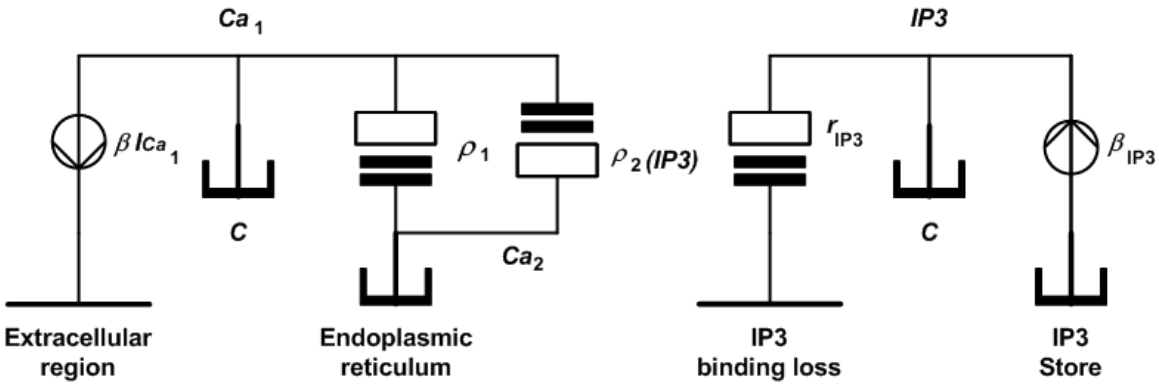

Figure 4.6: Simplified model of metabotropic-signal-induced calcium release.

As a final example we will consider a metabotropic signaling process in which internal Ca^{2+} stores are released from the endoplasmic reticulum to become free Ca^{2+} in the cytoplasm. Figure 4.6 illustrates the model. This model is intended to illustrate the general ideas conveyed by the qualitative models of this process. It should be noted that our present state of knowledge of the quantitative details of this process is incomplete and so the model presented here is to be regarded as conceptual but not an established accurate representation of this process.

The model contains two types of chemical concentrations, $[Ca^{2+}]_i$ represented on the left by node variable Ca_1, and cytoplasmic concentration of inositol triphosphate (IP_3) represented by node variable *IP3* on the right. Ca_2 represents the concentration of Ca^{2+} stored in the endoplasmic reticulum (ER). Typical concentrations of stored Ca^{2+} is typically greater than 100 μM under normal physiological conditions and likely reaches millimolar levels. The ER's supply of Ca^{2+} is by no means unlimited, but for normal signal processing functions we can regard the volume C_{ER} as effectively infinite so that concentration Ca_2 may be regarded as constant. We will also assume flux source $\beta \cdot I_{Ca1}$ includes a "leakage flux" that maintains the minimum level of Ca_1 at its resting concentration level (on the order of 50 to 100 nM). Transporter ρ_1 is the same as described previously. We will come back to transporter ρ_2 momentarily.

In the absence of synaptic metabotropic signaling, IP_3 is normally bound in the cytoplasmic membrane wall. It is liberated by the action of a membrane-spanning ***G-protein*** that acts as a receptor for metabotropic neurotransmitters. A G-protein receptor does not itself open to produce a pore for ionotropic current influx into the cytoplasm. Rather, it acts as a "molecular switch" to turn on the production of "second messenger" chemicals, IP_3 in this case. Flux source β_{IP3} models the generation of free IP_3 by this mechanism. The units of β_{IP3} are flux (moles per second).

Free IP_3 moves to the ER and binds with ***Ca-release channels*** in the membrane of the ER. As IP_3 again becomes bound by this process, it depletes the pool of free IP_3 and we can represent the

rate of this depletion using transporter r_{IP3}. Thus, the concentration *IP3* is described by[8]

$$C\frac{dIP3(t)}{dt} = -r_{\text{IP3}} \cdot IP3(t) + \beta_{\text{IP3}}. \tag{4.11}$$

Transporter $\rho_2(IP3)$ represents the influx of free Ca^{2+} due to the opening of the calcium-release channels in the ER. The kinetics of this process are complicated [MORA], but we can pose a few likely-seeming approximations. First, since the Ca^{2+} influx is zero in the absence of IP_3, the simplest plausible model for this effect is to presume the influx is proportional to $IP3(t)$. This assumption is analogous to that used in modeling calcium buffering in (4.9). Second, it is known that the opening probability, π_o, of the ER's calcium-release channels is strongly affected by the concentration level of cytoplasmic free calcium, Ca_1 [BEZP], [FINC], [MORA]. Bezprozvanny et al. report a bell-shaped curve function for release probability vs. $[Ca^{2+}]_i$ that reaches a peak of $\pi_o = 1$ at around $Ca_1 =$ 0.2 μM. The bell shape of the π_o dependency shows up on a logarithm plot of $[Ca^{2+}]_i$, i.e. the $\pi_o = 0.5$ points on the curve occur at approximately 0.075 μM and 0.55 μM [BEZP]. Bezprozvanny et al. report the fitted dependency as

$$\pi_o = \pi_s \frac{Ca_1^n \cdot k_1^n}{\left(Ca_1^n + k_2^n\right)\cdot\left(Ca_1^n + k_1^n\right)} \tag{4.12}$$

where π_s is a scale factor chosen to make π_o equal to 1 at $Ca_1 = 0.2$ μM, $n = 1.8$, $k_1 = k_2 = 0.2$ μM. Figure 4.7 graphs (4.12) as a function of calcium concentration Ca_1.

Taking these factors into account, we would write the transporter element law as

$$\rho_2 = \pi_o(Ca_1)\cdot \rho_{\max} \cdot IP3(t); \quad \phi_2 = \rho_2 \cdot Ca_2.$$

One noteworthy property of this system is the following. For concentrations Ca_1 less than about 0.2 μM, π_o is an *increasing* function of Ca_1, and thus there is a positive-feedback effect taking place inducing a strong rise in free cytoplasmic calcium. Above this level, π_o is a decreasing function of Ca_1, and so the total rise in free calcium is *self-inhibited* by the kinetics of the release probability. This has been known to produce *oscillations* in the concentration levels of free $[Ca^{2+}]_i$ in response to metabotropic signaling. This results in calcium-mediated *modulation* of ionotropic potassium currents [HILL5]. The oscillations are spike-like and very slow, with period

[8] There are other dynamics we are not representing accurately in this simplified model. For example, IP_3 does not remain indefinitely bound to the calcium-release channels, and this model depicts neither how long IP_3 remains bound (thus activating the channel) nor what happens to it later. An understanding of these additional dynamics is necessary for a complete and accurate model of this process [MORA]. The example given here is intended to merely illustrate an application of the Linvill model.

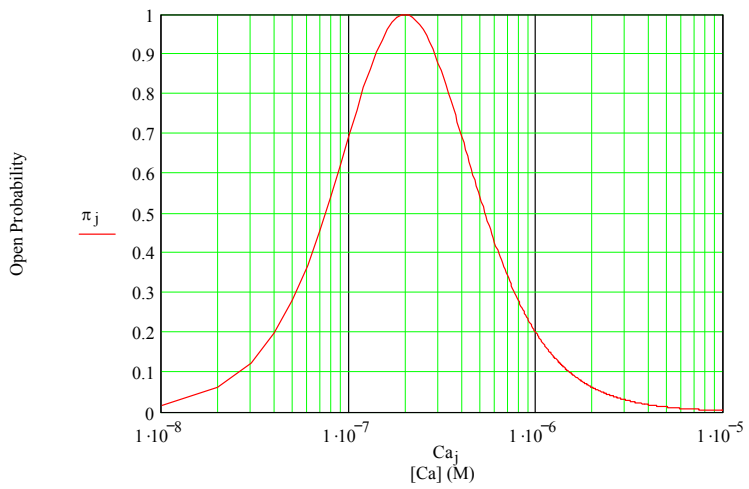

Figure 4.7: Empirical curve fit to calcium release channel open probability.

on the order of 12 to 20 seconds per spike for the case where IP_3 is produced in response to metabotropic action by the neuropeptide GnRH (gonadotropin-releasing hormone). Calcium spikes with peaks in the range of about 1.5 to 2.5 μM have been observed.

Summing effluxes from the Ca_1 node and incorporating (4.11) gives us the system of first order differential equations

$$\begin{bmatrix} dCa_1/dt \\ dIP3/dt \end{bmatrix} = \begin{bmatrix} -\rho_1/C & 0 \\ 0 & -r_{IP3}/C \end{bmatrix} \cdot \begin{bmatrix} Ca_1 \\ IP3 \end{bmatrix} + \begin{bmatrix} \rho_2/C & -\beta/C & 0 \\ 0 & 0 & 1/C \end{bmatrix} \cdot \begin{bmatrix} Ca_2 \\ I_{Ca_1} \\ \beta_{IP3} \end{bmatrix}. \qquad (4.13)$$

Although the equations in (4.13) appear to be uncoupled, in fact they are not. *IP3* couples into the first equation through ρ_2.

An additional consideration not incorporated into this simplified model would account for loss of free calcium through binding with the calcium-releasing channels depicted by ρ_2. The kinetics model of Moraru et al. [MORA] assumes two Ca^{2+} ions and four IP_3 molecules participate in each binding event at the receptor site for the calcium-releasing channels. This, however, could be taken into account in an approximate fashion by the numerical value assigned to ρ_2. More important is the absence in the simplified model of a time-dependent *rate process* description for transporters ρ_2 and r_{IP3}. In the simplest case we would have at least one additional differential equation, possibly similar to a rate process model such as is used in the Hodgkin-Huxley schema, capturing the opening- and closing-kinetics of the calcium releasing channels. Such a process would affect the time-dependencies of both ρ_2 and r_{IP3}. Judging from the findings reported in

[MORA], time constants for such a process would be on the order of a few milliseconds.

As a final note, the model just presented is a very simplified representation of these dynamics. Much more elegant treatments based on diffusion theory and partial differential equation models have been formulated [DeSC]. A lumped model approximation for this type of sophisticated model would require the model of Figure 4.6 to be turned into a multi-compartment model.

§ 2.5 Calcium-activated Potassium Channels

An important class of channels not yet discussed is the calcium-activated K^+ voltage-gated channel. There are at least two important signaling sub-classes of Ca^{2+} activated K^+ channels, which we will denote by currents $I_{K(Ca)}$ and $I_{K(AHP)}$. The latter is further subdivided into the categories "intermediate channel" (IK) and "small channel" (SK). The first type, correspondingly, is often called the "big channel" (BK).

Empirical models for the various denizens of the "zoo" of K^+ channels are often expressed in terms of the steady-state activation variable, m_∞, and a time constant, τ_m. Assuming, as did Hodgkin and Huxley, that channel activation follows a first-order rate process, the activation variable is described by the difference equation

$$m(t+\Delta t) = m_\infty - (m_\infty - m(t)) \cdot \exp(-\Delta t/\tau_m). \tag{4.14}$$

m_∞ is typically described either in terms of Hodgkin-Huxley rate parameters, α and β, or else in terms of a Boltzmann equation

$$m_\infty = \frac{1}{1+\exp[(V_{50} - V_m)/k]}. \tag{4.15}$$

While the BK class of channels is both voltage- and calcium-dependent, the IK and SK classes are not strongly voltage dependent and therefore do not follow the form (4.15). Their primary effect is to produce a long-lasting hyperpolarization (the "after-hyperpolarization") following intense spiking activity by the neuron, but they also modulate the resting potential and excitability of the neuron in response to IP_3-producing metabotropic signaling.

Yamada et al. [YAMA] presented a BK model derived from the sympathetic ganglion B-type cell of the bullfrog. (McCormick and Huguenard also used this same model in [McCO]). The current equation for their model is

$$I_{K(Ca)} = g_{\max} \cdot m \cdot (V_m - E_K) \tag{4.16}$$

with the auxiliary equations

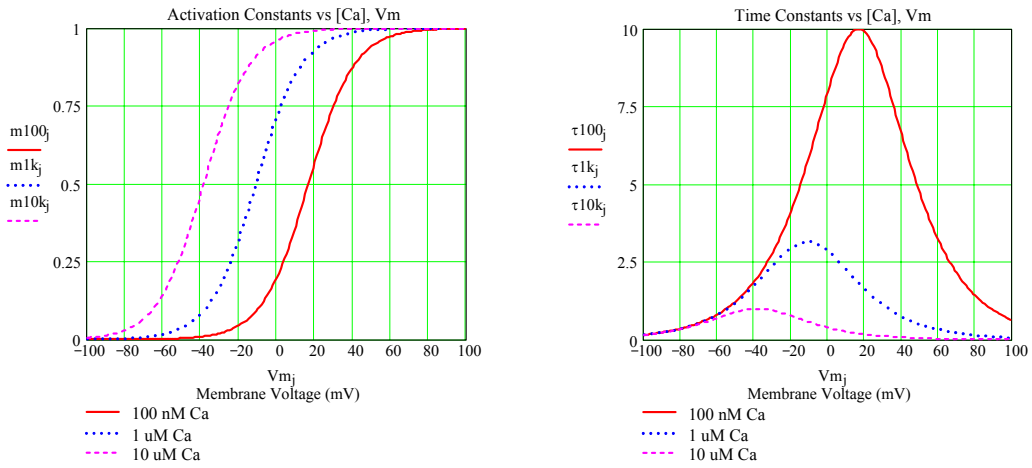

Figure 4.8: Steady-state activation constants and time constants for $I_{K(ca)}$ vs. calcium concentration.

$$\frac{dm}{dt} = \frac{m_\infty - m}{\tau_m}$$

$$\tau_m = \frac{1}{250 \cdot \left[Ca^{2+}\right]_i \cdot \exp\left(V_m/24\right) + 0.1 \cdot \exp\left(-V_m/24\right)} \quad . \qquad (4.17)$$

$$m_\infty = \tau_m \cdot 250 \cdot \left[Ca^{2+}\right]_i \cdot \exp\left(V_m/24\right)$$

In these expressions, $[Ca^{2+}]_i$ is in mM and V_m is in mV. The time constant is in ms. Yamada et al. gave g_{max} as 1.2 μS. Figure 4.8 illustrates the dependency of the steady-state activation constant, m_∞, and time constant, τ_m, on $[Ca^{2+}]_i$ as a function of membrane potential. At normal resting levels of Ca^{2+} (around 100 nM) the calcium-dependent K channel is effectively closed at the resting potential (around –65 to –60 mV) and the channel time constant during action potential generation is slow in comparison with its values for elevated Ca^{2+} levels. Increasing the cell's internal concentration of Ca^{2+} shifts the activation curve to more negative membrane potentials, and the maximum time constant falls dramatically.

An $I_{K(AHP)}$ model was also presented in [YAMA]. This after-hyperpolarization current (that is, the after-hyperpolarization that occurs following the generation of an action potential) is not a strong function of membrane potential. Rather, it is a potassium channel current that depends on the internal concentration of Ca^{2+}. Yamada et al. give the current equation as

$$I_{K(AHP)} = g_{max} \cdot m^2 \cdot \left(V_m - E_K\right) \qquad (4.18)$$

with a maximum channel conductance g_{max} of 0.054 μS. The differential equation for m is the same as for the Ca-dependent BK current channel but the expressions for the calcium dependency are different and are given by

$$\tau_m = \frac{1000}{1.25 \cdot 10^8 \cdot \left[Ca^{2+}\right]_i^2 + 2.5}$$
$$m_\infty = \tau_m \cdot 1.25 \cdot 10^5 \cdot \left[Ca^{2+}\right]_i^2 \qquad (4.19)$$

where the calcium concentration is given in mM and the time constant is in ms. At resting levels of calcium (around 100 nM = 10^{-4} mM), the time constant is on the order of 300 ms. This leads to very long after-hyperpolarization "tails" following the generation of an action potential, and therefore contributes to a longer relative refraction period for the neuron.

§ 3. Other Modulating Currents

The section just concluded illustrates the many ways in which various specialized voltage-gated and calcium-dependent channels contribute to the overall activity characteristics of the neuron according to the Hodgkin-Huxley modeling schema. These channels, by going beyond the comparatively simple axon dynamics first explained by Hodgkin and Huxley, are what make the neuron's signal processing characteristics far more sophisticated than those of the simple axon. Stepping back a bit from the details, a general theme can be formulated from what we have seen so far: The unique signal processing properties of specific neuron types is due to the neuron's "equipment" of a suite of ionotropic channels with specific voltage-current-calcium characteristics. No discussion of the signal processing functions of a neuron is complete without a treatment of these modulating channels.

§ 3.1 The Delayed Rectifier K Channel

The non-inactivating K-current in the Hodgkin-Huxley axon model was responsible for rapid repolarization of the membrane following an action potential. Somewhat surprisingly, this current appears to not play this same role in the cell body of the neuron itself. Rather, in many cases this role is played instead by $I_{K(Ca)}$. In its place, another outward-flowing "delayed rectifier" current is often found in the neuron's cell body. This current is a slowly inactivating K-current, usually called the I_K current but sometimes called the I_{K2} current (e.g. in [HUGU]). It seems likely that this name is actually a label for a possibly large number of slightly different K^+ VGCs. The primary role of this current in the neuron is likely to be the moderation of low-threshold calcium currents (T-currents), probably retardation of the approach of V_m to the firing threshold, and possibly an affect on the rapidity with which action potentials may be generated.

Huguenard and McCormick [HUGU] and Yamata et al. [YAMA] provide different model expressions for this current. This is most likely due to diversity in this species of channel than anything else. As the Yamata et al. model is slightly simpler, it is presented here.

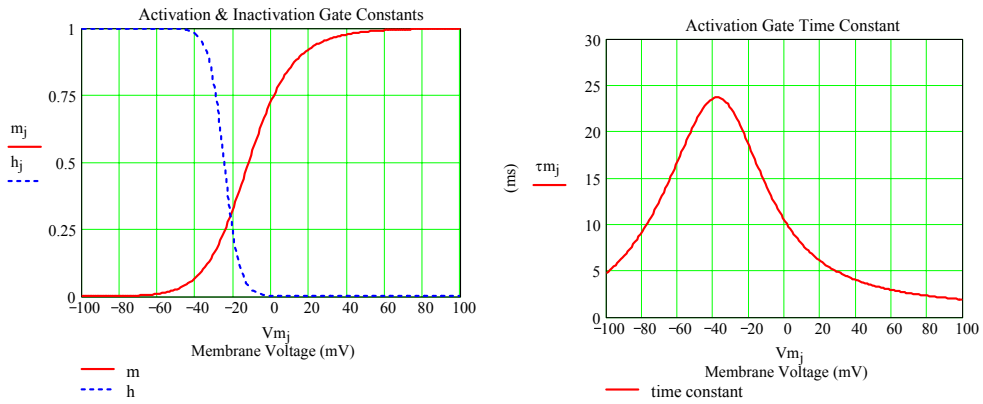

Figure 4.9: Activation and inactivation variables for the slow delayed rectifier channel. The inactivation gate time constant is 6000 ms for V_m < –20 mV and 50 ms otherwise.

The expression for I_K is very similar to the Hodgkin-Huxley expression except for the presence of an inactivation gate variable, h,

$$I_K = g_{K\max} \cdot m^2 h \cdot (V_m - E_K). \tag{4.20}$$

They give 0.084 μS as the value for the maximum conductance $g_{K\max}$. The differential equations for the gating kinetics are described in standard form,

$$\frac{dm}{dt} = \frac{m_\infty - m}{\tau_m}; \qquad \frac{dh}{dt} = \frac{h_\infty - h}{\tau_h}. \tag{4.21}$$

The activation gate is described in terms of Hodgkin-Huxley-like rate variables, α_m and β_m, with

$$\begin{aligned} \alpha_m(V_m) &= \frac{-0.0047 \cdot (V_m + 12)}{\exp(-(V_m + 12)/12) - 1} \\ \beta_m(V_m) &= \exp(-(V_m + 147)/30) \end{aligned}. \tag{4.22}$$

The activation gate time constant is given by the usual expression, $\tau_m = 1/(\alpha_m(V_m) + \beta_m(V_m))$. What is interesting here is that the steady-state activation, m_∞, uses a *shifted* membrane potential,

$$m_\infty = \tau_m(V_m - 20) \cdot \alpha_m(V_m - 20).$$

This is, of course, equivalent to subtracting 20 mV from the constants added to V_m in (4.22). As usual, the unit of V_m is mV in these expressions.

The inactivation gate is interesting in that its time constant is indeed constant, although a bi-phasic function of V_m. For V_m < –25 mV, τ_h = 6,000 ms (6 seconds). Otherwise, for membrane potentials at and above –25 mV, τ_h = 50 ms. I_K is indeed a *slowly* inactivating current*!* The steady-state inactivation variable is given by a simple Boltzmann equation expression,

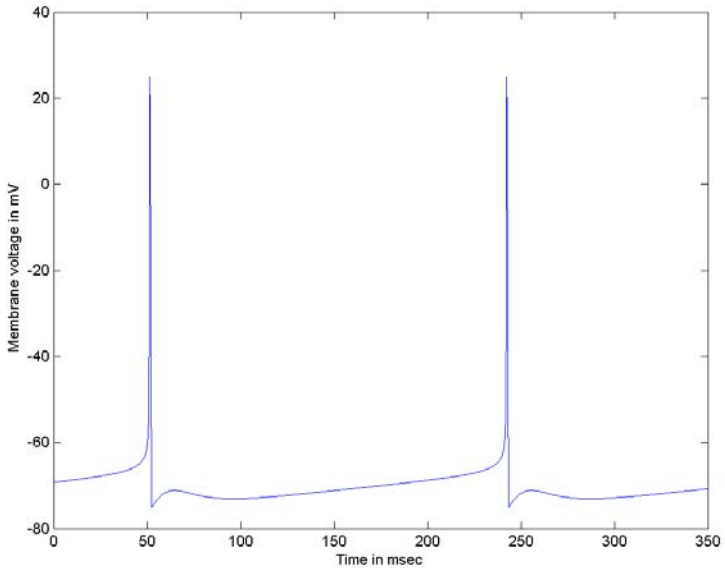

Figure 4.10: Illustration of repetitive firing in a cortical neuron.

$$h_{\infty} = \frac{1}{1+\exp\left(+\left(V_m+25\right)/4\right)} \ . \tag{4.23}$$

The steady-state gate kinetics are shown in Figure 4.9.

§ 3.2 The A-current K Channel

Another potassium modulation current widely found in neurons is a rapidly-activating/slowly-deactivating transient current commonly called the "A" current, I_A. The channel is frequently called the K_A channel. This interesting channel is activated by depolarization and then quickly inactivates. One of its most notable features is that it remains largely inactivated at the normal resting potential of the neuron. A strong hyperpolarization of the cell is required to remove the inactivation, after which I_A causes a delay in the generation of the action potential and an increase in the firing threshold for subsequent action potentials until the channel's inactivation catches up.

K_A contributes to repetitive firing in neurons that strongly hyperpolarize after an action potential. Hyperpolarization removes the inactivation of the K_A channel, which helps to hold V_m at a hyperpolarized value. However, as the channel subsequently slowly inactivates, the membrane potential can build back up, which increases the amount of K_A inactivation. If the other channels are capable, in the absence of I_A, of charging V_m past the firing threshold, another action potential is generated. The subsequent hyperpolarization again removes the I_A inactivation and the cycle begins anew. Figure 4.10 illustrates an example of this firing behavior in a model cortical neuron. It should be noted that this type of repetitive firing is not due to the A current

alone. It is sometimes mechanized by interaction between the A current and a T-type LVA Ca^{2+} current, although this is not a universal rule by any means. One can also note that the term "resting potential" becomes somewhat equivocal in the case of a neuron that fires repetitively (and is therefore never "at rest").

Different researchers have reported different parameter values for K_A channels. This term is a label for a species of Kv (delayed rectifier) channels, and so the diversity in the literature is not surprising. Huguenard and McCormick [HUGU] reported an I_A model in which they were led to develop two independent K_A channels. Yamada et al. [YAMA] and Connor and Stevens [CONN1-2] each reported a single K_A channel, but their parametric values are considerably different from one another and from [HUGU]. The generic model formula for I_A is

$$I_A = g_{A\max} \cdot m^N \cdot h \cdot (V_m - E_K) \tag{4.23}$$

with N usually equal to either 3 or 4, although Yamada et al. reported an $N = 1$ model.

Both m and h are usually described in the form of difference equation (4.14) with m_∞ and h_∞ both described by a Boltzmann equation (4.15). In [HUGU] the two A channels were fitted with the Boltzmann equation parameters shown in table 4.1. In their model, $N = 4$.

TABLE 4.1

variable	Channel A_1	Channel A_2
m_∞	$V_{50} = -60$ mV $k = 8.5$ mV	$V_{50} = -36$ mV $k = 20$ mV
h_∞	$V_{50} = -78$ mV $k = -6.0$ mV	$V_{50} = -78$ mV $k = -6.0$ mV

Model expressions for the time constants also show a great deal of diversity in the literature. Many researchers note that measurements show a large amount of variance and deal with this by setting both τ_m and τ_h equal to constant values. τ_m values in the range from 0.5 to 2.5 ms are fairly typical. τ_h frequently appears to be biphasic with values of 50 to 150 ms below $V_m = -80$ to -63 mV and τ_h in the range of 20 ms being common for V_m greater than this biphasic threshold value. [HUGU] did report a functional description rather than a constant value for these parameters. Their model values for $g_{A\max}$ were 0.5 to 2.4 μS with an average of 1.2 μS in [McCO].

§ 3.3 The M-current K Channel

Another important class of modulating potassium channel is the K_M or "M-current" channel. It is a slowly-activating, non-inactivating (persistent) channel. Near the resting potential of the neuron its time constant for activation is typically a few hundred ms. Thus, this current is not

thought to have much affect on the generation of a single action potential, but it is thought to contribute to slowing down the firing rate of the neuron (**accommodation** of firing rate) during long, sustained burst-firing activity. Yamada et al. [YAMA] reported a steady state activation function m_∞ described by (4.15) with Boltzmann function parameters $V_{50} = -35$ mV and $k = 10$ mV. The time constant function was described by

$$\tau_m = \frac{1000}{3.3 \cdot \left[\exp\left(+\left(V_m + 35\right)/40\right) + \exp\left(-\left(V_m + 35\right)/20\right)\right]} \ . \tag{4.24}$$

The expression for the M-current was

$$I_M = g_{M\max} \cdot m \cdot \left(V_m - E_K\right) \tag{4.25}$$

with $g_{M\max} = 0.084$ μS.

However, probably the most important modulation feature of the M-current is its sensitivity to metabotropic input signals. A variety of neuromodulators [BROW], [MARR] are known to inhibit the M-current, effectively taking its conductance to zero. As I_M is a potassium current, this action tends to raise the resting potential of the cell and has been known to contribute to producing ***burst firing*** rather than a single action potential response to a stimulus. Figure 4.11 illustrates this type of response activity for a cortical neuron model. Other neuromodulators are known to enhance the M-current, thereby producing hyperpolarization of the cell with an accompanying decrease in the excitability of the cell.

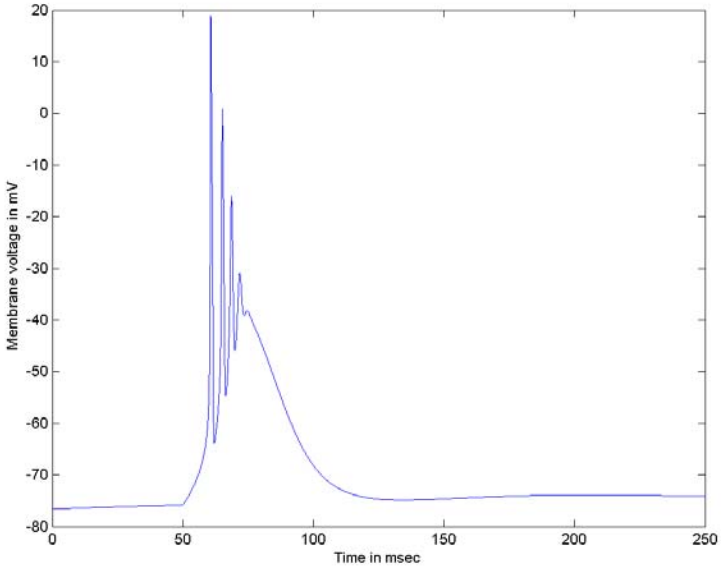

Figure 4.11: Bursting response in a cortical neuron.

Responses such as that illustrated in Figure 4.11 are typically measured at the cell body (soma). From the discussion earlier in this text on the presynaptic threshold level mentioned in the context of neurotransmitter release at a synapse, it is appropriate to remark about something here that is potentially misleading about the action potential response of this cell. It was earlier stated that the threshold for neurotransmitter exocytosis is in the range of about –30 to –20 mV, the activation levels of HVA calcium channels found in the neuron's presynaptic terminal. Figure 4.11 therefore appears to imply that only the first two or three action potential responses will be effective in stimulating neurotransmitter release. However, one should also remember that *axons* typically have a more hair-trigger response to stimulus than does the cell body. Current flowing into the axon as a result of depolarization of the soma might, therefore, stimulate AP responses in the axon merely from the depolarization of the soma and not necessarily from only the soma's action potential spikes. Detailed quantitative modeling of the soma-axon interaction requires a multi-compartment model, treating the soma and dendrites of the cell as one compartment and the axon as another with a resistive series connection between their respective Hodgkin-Huxley compartments. Furthermore, since current flow in an axon is generally unidirectional (owing to the refractory period of the axon), this resistive connection most likely would have to be a rectifying connection, which is to say it must allow current flow from the soma to the axon but not the reverse. Thus, the series connection resistance must be a nonlinear function of the potential difference across it, $V_{m\,\mathrm{soma}} - V_{m\,\mathrm{axon}}$. Electrical engineers call this sort of *I-V* relationship ***diode action***. The simplest model for this is $I_{series} = G_{series} \cdot (V_{m\,\mathrm{soma}} - V_{m\,\mathrm{axon}}) \cdot \mathrm{H}(V_{m\,\mathrm{soma}} - V_{m\,\mathrm{axon}})$, where H(•) is the Heaviside function. A slightly more complex model adds a threshold value to the argument of H, e.g. $\mathrm{H}(V_{m\,\mathrm{soma}} - V_{m\,\mathrm{axon}} - V_{thresh})$ where V_{thresh} is non-negative.

§ 3.4 Hyperpolarization-activated Mixed-cation Channels

As the last example of voltage-gated channel diversity, we consider the hyperpolarization-activated mixed-cation channel. These channels conduct both Na^+ and K^+ ions. Consequently, the associated battery potential is neither E_{Na} nor E_K but, presumably, a Thévenin equivalent potential, V_h, combining the two. These channel currents are typically called "h-currents" although "h" here has nothing to do with the Hodgkin-Huxley inactivation variable. However, the activation curve for m vs. V_m does resemble that of the H-H inactivation variable. The channel current is described by

$$I_h = g_{\max} \cdot m \cdot \left(V_m - V_h\right) .$$

The h-current is an inward rectifying current since these channels conduct current into the

cytoplasm readily but do not conduct outward current flows. The physiological explanation for this rectifying action is that the h-channel is normally blocked from the cytoplasmic side by a Mg^{2+} ion. Hyperpolarization of the membrane potential is required to remove this blocking particle from the channel and allow conduction. These channels can also be blocked by Cs^{+} and Rb^{+} [HILL4: 158].

Huguenard and McCormick [HUGU] modeled their h-channel in the thalamocortical relay neuron using a Boltzmann function (4.15) for m_∞ with parameters V_{50} = –75 mV and k = –5.5 mV. They obtained an expression for the time constant by fitting a bell-shaped function to their data, obtaining

$$\tau_m = \frac{1}{\exp(-14.59 - 0.086 \cdot V_m) + \exp(-1.87 + 0.0701 \cdot V_m)} \ .$$

They reported a value of V_h = –43 mV with g_{max} between 10 and 30 nS for their model [McCO].

Because the h-current is largely deactivated for voltages near the resting potential and becomes fully activated for hyperpolarizations of $V_m \cong$ –90 mV and less, its role in signal processing is not entirely clear. It is usually agreed that they play a part in determining the cell's resting potential. Because the time constant is large, these channels produce long, slow recoveries after hyperpolarization to the resting potential. They are also known to be responsive to the metabotropic second messenger chemical cyclic AMP (cAMP), and therefore their depolarizing effect is directly responsive to metabotropic signaling processes that produce cAMP within the neuron.

§ 4. Ionotropic Synapse Channels

Chapter 3 provided a generic discussion of channel modeling for synapses. In this section more specific characteristics of the principal ionotropic channels are presented. There are three primary channel types that take in the majority of all ionotropic synaptic signaling in the central nervous system. Two of these, the NMDA channel and the AMPA channel, are excitatory. The third, the $GABA_A$ channel, is inhibitory.

The distribution of synaptic channel types in the neuron follows a general trend. In mammals all excitatory synapses (NMDA and AMPA) occur on the dendrites of the neuron. In contrast, only 31% of inhibitory synapses occur on dendrites, and these tend to be found near the cell body. The remaining 69% of inhibitory synapses occur on the cell body itself. This geographic arrangement places the inhibitory synapses in a position to block the effects, in whole or in part, of the more remote excitatory input signals. In many neurons, but by no means in all, the dendrites lack voltage-gated Na^{+} channels, and so in these cases no action potentials are generated

out in the dendrites. Thus, the inhibitory $GABA_A$ channels need not cope with the large-signal levels associated with AP production, and need only deal with the much lower-level excitatory postsynaptic potentials and currents (EPSPs and EPSCs) produced by excitatory synapses.

Neurons are broadly classified as ***spiny*** and ***nonspiny***. Examples of spiny neurons include the pyramidal cell and the spiny stellate cell in the neocortex and the Purkinje cell in the cerebellum. Pyramidal cells and spiny stellate cells are the excitatory neurons of the neocortex and make up roughly 85% of all neurons in the neocortex (65% pyramidal cells, 20% spiny stellate cells). In contrast, the cerebellar Purkinje cell is an inhibitory neuron and serves as the principal output cell for the cerebellum. A ***spine*** is a small protrusion from the dendrite. Spines greatly increase the amount of surface area on a dendrite, and the majority of excitatory synapses occur on spines. (This is true for all three of the cells just introduced). Inhibitory synapses occurring on the dendrites of spiny cells occur mainly on the dendritic shaft. Spines are dynamic structures that grow and disappear in response to synaptic activity and to metabotropic activity produced within the neuron by various chemical "secondary effectors" including Ca^{2+} release by the ER [LÜSC]. The principal neurotransmitter for an excitatory synapse is glutamate (Glu).

Nonspiny cells make up the remaining 15% of all neurons in mammalian neocortex. The non-spiny neocortical cells are inhibitory neurons. Their excitatory synapses form on the dendritic shafts. Like the spiny neurons, the postsynaptic receptors at excitatory synapses are glutamate receptor proteins (GluRs). In contrast to the excitatory neurons, which secrete Glu at their presynaptic terminals, the principal inhibitory neurotransmitter secreted by these cells is gamma-aminobutyric acid (GABA). The principal ionotropic receptor at inhibitory synapses is called the $GABA_A$ receptor, to distinguish it from a metabotropic GABA receptor protein called $GABA_B$.

§ 4.1 The NMDA Channel

The N-methyl-D-aspartate or NMDA channel is perhaps the most scientifically interesting of all the ionotropic synaptic channels. Not only does it stand in a class by itself as a signal processing mechanism; it is also implicated in long-term synaptic plasticity, which in turn is thought to be the physiological basis for learning and memory.

NMDA channel proteins bind with glutamate and form excitatory ionotropic channels. There are two primary peculiarities found in NMDA channels. First, these channels are normally blocked from the extracellular side by Mg^{2+} particles and depolarization of the membrane potential is required to eject the Mg^{2+} and open the channel pore. Thus one says the NMDA channel is ***glutamate enabled – voltage activated***. Its *I-V* characteristic is therefore a function of the level of *extracellular* Mg^{2+} concentration as well as membrane potential V_m.

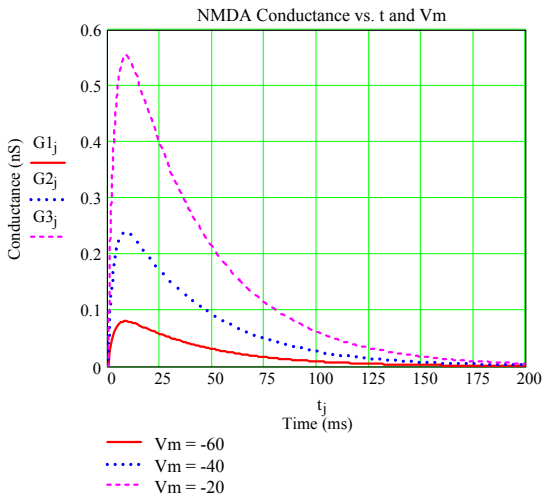

Figure 4.12: NMDA channel conductance vs. time and membrane potential.

The second peculiarity of the NMDA channel is that it conducts Ca^{2+} as well as both Na^{+} and K^{+}. In the physiological range of neuron operation, the Ca^{2+} and Na^{+} currents flow into the cytoplasm, while the K^{+} current flows out of the cytoplasm. The total I_{NMDA} current is the sum of all three components (regarding the K^{+} component as being opposite in sign to the other two). It is known that most of the current conducted by the NMDA channel is due to Ca^{2+}, and so this channel is usually referred to as a calcium channel.

The NMDA channel slowly desensitizes following the binding of the Glu neurotransmitter. The time constant for deactivation of this channel is on the order of about 40 ms. The time course of its channel conductance is most often described by a beta-function (chapter 3, equations 3.20 through 3.25). Because the channel is membrane-voltage-dependent, the usual beta-function expression must be slightly modified and the channel conductance is expressed as [GABB]

$$G_{syn}(t) = g_{NMDA}\frac{\gamma}{1+\left[Mg^{2+}\right]_o \exp(-\alpha V_m)/\beta}\cdot\left(\exp(-t/\tau_2)-\exp(-t/\tau_1)\right)\mathrm{H}(t) \qquad (4.26)$$

where H(t) is the Heaviside function and

$$\gamma = \frac{1}{\exp(-T_{pk}/\tau_2)-\exp(-T_{pk}/\tau_1)}, \quad T_{pk} = \frac{\tau_1\tau_2}{\tau_2-\tau_1}\ln\left(\frac{\tau_2}{\tau_1}\right)$$

as before. The extracellular Mg^{2+} concentration has a typical value of 1.2 mM, and the other parameters have the corresponding values β = 3.57 mM, α = 0.062/mV, τ_1 = 3 ms, τ_2 = 40 ms. Gabbiani et al. give a maximum conductance (per synapse) parameter g_{NMDA} = 1.2 nS. With these parameter values, γ = 1.34261. Figure 4.12 illustrates $G_{syn}(t)$ using these parameters for three

membrane potentials. The NMDA current is given by

$$I_{NMDA} = G_{syn}(t) \cdot (V_m - E_{syn})$$

with E_{syn} = 0 mV for this synaptic channel. In a dynamical simulation, (4.26) would be replaced by the difference equation calculation as discussed in chapter 3 using equations (3.20) through (3.25) and with γ being replaced by the modified term in (4.26).

The distribution of locations for synapses containing NMDA receptors in the central nervous system is still not fully explored. Most neurons have NMDA, as well as non-NMDA, receptors. Most, perhaps all, excitatory synapses in pyramidal and spiny stellate cells in the forebrain contain NMDA receptors in their dendritic spines. On the other hand, NMDA receptors are absent from the spines in mature cerebellar Purkinje cells. There is even evidence that NMDA receptors exist in the presynaptic terminals of at least some neurons and play a role in modulating neurotransmitter release [COCH], [GLIT].

Because free cytoplasmic Ca^{2+} is such a potent chemical messenger and is implicated in many biochemical reactions inside the cell, the existence of Ca^{2+}-conducting synaptic channels has many profound implications. It is well established that Ca^{2+} is implicated in long term potentiation and long term depression in the response of a cell to glutaminergic signaling. It is also involved in phosphorylation/dephosphorylation processes that modulate the sensitivity of other channels, e.g. the Ca^{2+}-dependent K^+ channels. Because the NMDA channel requires a "voltage assist" to remove the Mg^{2+} blocking particle and allow current flow, the opening of NMDA channels is heavily correlated with signals at other non-NMDA glutamate receptors. Thus, the NMDA channel is often regarded as a **coincidence detector** that responds only when sufficient synaptic activity involving non-NMDA glutamate receptors exists.

§ 4.2 The AMPA Channel

AMPA receptors constitute the principal non-NMDA ionotropic synaptic channel responding to glutamate.[9] The AMPA ligand-gated channel differs from the NMDA channel in three important respects. First, the AMPA channel conducts a Na^+ current into the cell (and allows the passage of a lesser amount of K^+ current efflux) but does not conduct Ca^{2+}. The AMPA current is described by

$$I_{AMPA} = G_{AMPA}(t) \cdot (V_m - E_{syn})$$

[9] There is another glutamate-responding ligand-gated channel known as the Kainate (KA) channel. From a signal processing perspective, the KA channel and the AMPA channel behave in much the same way and we will not treat the KA channel separately.

with $E_{syn} = 0$. G_{AMPA} is not membrane-voltage sensitive. Third, the AMPA channel responds much more quickly to gating by Glu than does the NMDA channel. G_{AMPA} has been described by both the beta-function,

$$G_{AMPA} = g_{\max} \cdot g^{(\beta)}(t), \qquad \text{(chapter 3, equations 3.20 to 3.25)}$$

and the alpha-function,

$$G_{AMPA} = g_{\max} \cdot g^{(\alpha)}(t), \qquad \text{(chapter 3, equations 3.15 to 3.19).}$$

For example, Gabbiani et al. [GABB] used a beta-function description with $g_{\max}$ = 720 pS and time constants $\tau_1 = 0.09$ ms and $\tau_2 = 1.5$ ms.

AMPA channels are often co-localized with NMDA channels within the same synapse. In these cases, the total synaptic conductance is $G_{syn} = G_{AMPA} + G_{NMDA}$. One interesting phenomenon in this regard is the finding that the number of AMPA receptors co-localized with NMDA receptors appears to be activity dependent, and their relative density can change over relatively short time scales [LÜSC], [MALE]. This has led to a well-supported hypothesis that a "pool" of AMPA receptors is available from which the receptor proteins can be relocated to the membrane wall of the synapse. Their insertion or deletion modifies the $g_{\max}$ of the AMPA channel, and is thus one possible mechanism for activity-dependent modulation of the "strength" of the synaptic response. (Signal processing researchers often refer to this as **adaptation of the synaptic weight** of the neuron). The relative density of AMPA to NMDA receptors co-localized in one synapse is experimentally found to range from zero (no AMPA activity, the so-called "silent synapse") to much greater than one (AMPA-dominated synapses).

§ 4.3 The GABA Channel

The principal inhibitory ligand-gated channel (LGC) in the central nervous system uses the neurotransmitter GABA (gamma-aminobutyric acid) and the $GABA_A$ class of receptor protein. The GABA channel primarily conducts chloride and is modeled using an E_{syn} in the range of –70 to –75 mV. GABA LGC conductance is often described by an alpha-function with a time constant of 5 ms, although the synapses on cerebellar granule cells to which the cerebellum's Purkinje cells project are also known to have a second "slow" current component with a fast rise-time constant (τ_1) and a slow decay-time constant (τ_2) on the order of 50 ms. (The slow component therefore must be described by a beta-function rather than an alpha function). For those GABA channels described by an alpha-function, a typical $g_{\max}$ is in the range of 10 to 30 pS per pore and from about 0.25 to 1.2 nS per synapse [DEST].

In addition to the GABA channel, there is another inhibitory LGC known as the glycine

channel. From the point of view of signal processing, there is little distinction between the two channels (although, of course, to the physiologist they are quite distinct). In this text we will not further distinguish between these two types of inhibitory LGCs.

§ 4.4 Multiple Synapses and Synaptic Weight

While one could model each individual synapse with its own characteristic E_{syn} battery and G_{syn} conductance, the large number of synapses on a typical neuron make this simple approach computationally impractical. Each synapse would add two more difference equations to the neuron model, and each additional difference equation requiring solution increases the cost of the computation.

Fortunately, this cost explosion is wholly unnecessary because the difference equations describing the phenomenological form of synaptic input are linear equations. Whether the dynamics are expressed by an alpha function,

$$\begin{bmatrix} x_1(t+\Delta t) \\ x_2(t+\Delta t) \end{bmatrix} = \begin{bmatrix} 1-\Delta t/\tau & 0 \\ \Delta t & 1-\Delta t/\tau \end{bmatrix} \begin{bmatrix} x_1(t) \\ x_2(t) \end{bmatrix} + \begin{bmatrix} \nu \\ 0 \end{bmatrix} \mathrm{H}\left[V_{pre}(t)-\Omega\right] \quad (3.18)$$

$$g^{(\alpha)}(t) = \begin{bmatrix} 0 & \exp(1)/\tau \end{bmatrix} \begin{bmatrix} x_1(t) \\ x_2(t) \end{bmatrix} \quad (3.19)$$

or by a beta function

$$\begin{bmatrix} x_1(t+\Delta t) \\ x_2(t+\Delta t) \end{bmatrix} = \begin{bmatrix} 1-\Delta t/\tau_1 & 0 \\ 0 & 1-\Delta t/\tau_2 \end{bmatrix} \begin{bmatrix} x_1(t) \\ x_2(t) \end{bmatrix} + \begin{bmatrix} \nu \\ \nu \end{bmatrix} \mathrm{H}\left[V_{pre}(t)-\Omega\right] \quad (3.25)$$

$$g^{(\beta)}(t) = \begin{bmatrix} -\gamma & \gamma \end{bmatrix} \begin{bmatrix} x_1(t) \\ x_2(t) \end{bmatrix} \quad (3.24)$$

the *net* synaptic current due to all synapses of the same type at any time t can be found by summing the inputs of every synapse for which $\mathrm{H}[V_{pre}(t) - \Omega] = 1$. To a reasonable statistical approximation, this can be done through the ν factor in (3.18) or (3.25) in the following way.

Let n_{syn} be the number of synapses a neuron has of a particular type (e.g. NMDA synapses). Let g_0 represent the average maximum conductance parameter for synapses of this type. The maximum conductance of synapse n can then be represented by a non-negative weighting factor, w_n such that $g_{\max(n)} = g_0 \cdot w_n$. Numbering the neuron's synapses from 1 to n_{syn}, the distribution of ***synaptic weights*** can then be represented by a column ***weight vector***,

$$W^T = \begin{bmatrix} w_1 & w_2 & \cdots & w_{n_{syn}} \end{bmatrix} \quad (4.27)$$

where T denotes the transpose of the vector. The distribution of maximum conductances is clearly given by the product $g_0 \cdot W$ and we can let g_0 take the place of $g_{\max}$ in the expression for G_{syn}.

Now let $Q(t)$ denote the vector Heaviside function of all synaptic inputs of this type, i.e.,

$$Q^T(t) = \left\lfloor \quad \mathrm{H}\left(V_{pre_1}(t) - \Omega_1\right) \qquad \mathrm{H}\left(V_{pre_2}(t) - \Omega_2\right) \qquad \cdots \qquad \mathrm{H}\left(V_{pre_{nsyn}}(t) - \Omega_{nsyn}\right) \right\rfloor. \quad (4.28)$$

The net contribution to the total synaptic conductance at time t is given by the sum of all the synaptic inputs for which the Heaviside functions are non-zero. This can be represented by

$$\nu(t) = W^T Q(t) \quad (4.28)$$

so that equations (3.18) and (3.25) become

$$\begin{bmatrix} x_1(t+\Delta t) \\ x_2(t+\Delta t) \end{bmatrix} = \begin{bmatrix} 1-\Delta t/\tau & 0 \\ \Delta t & 1-\Delta t/\tau \end{bmatrix} \begin{bmatrix} x_1(t) \\ x_2(t) \end{bmatrix} + \begin{bmatrix} 1 \\ 0 \end{bmatrix} \nu(t) \quad (4.29)$$

$$\begin{bmatrix} x_1(t+\Delta t) \\ x_2(t+\Delta t) \end{bmatrix} = \begin{bmatrix} 1-\Delta t/\tau_1 & 0 \\ 0 & 1-\Delta t/\tau_2 \end{bmatrix} \begin{bmatrix} x_1(t) \\ x_2(t) \end{bmatrix} + \begin{bmatrix} 1 \\ 1 \end{bmatrix} \nu(t) \quad (4.30)$$

respectively.

One vector product (4.28) and one pair of state equations (4.29) or (4.30) must be used for each unique synapse type (NMDA, AMPA, or $GABA_A$) for a single-compartment neuron model of the Hodgkin-Huxley type. Thus, the total additional computational cost for modeling synaptic inputs is limited to at most six difference equations and three vector products regardless of how many synapses the neuron may have.

§ 5. Glial Cells

In the 60+ years of neural network research, it has always been the traditional presupposition that neurons alone are responsible for biological signal processing. Since the late 1980s this tradition has come under increasing scrutiny by physiologists conducting research on glial cells in the central nervous system. There is mounting evidence that glia in central systems are not the passive and, from a signal processing viewpoint, uninteresting cells the traditional view has held them to be. Do glial cells participate in biological signal processing by neurons? The scientific verdict has not yet been definitively delivered on this question, but there is now ample evidence telling us we may not simply dismiss glial cells from the picture as tradition has long done. The new evidence makes all the more prescient a remark made in 1899 by pioneer and Nobel laureate Santiago Ramón y Cajal:

> The prejudice that the relation between neuroglial fibers and neuronal cells is similar to the relation between connective tissue and muscle or gland cells, that is, a passive weft for merely filling and support (and in the best case, a gangue for taking nutritive juices), constitutes the main obstacle that the researcher needs to remove to get a rational concept about the activity of the neuroglia.

Glial cells outnumber neurons in human brain by on the order of 10:1. Glial cells, particularly the star-shaped glial cells called ***astrocytes***, are intimately associated with synapses, ensheathing up to a few thousand synapses per astrocyte. Glial cells are themselves interconnected in a vast network of cells, the ***glial syncytium***, joined by gap junction synapses. They also possess many of the same or similar types of ionotropic and metabotropic channels as neurons do, although the density of Na^+ and Ca^{2+} channels is insufficient to cause large-amplitude spiking of the glial cell's membrane potential [VERK], [BARR1-2]. It is the very inactivity of the glial cell's membrane potential that led researchers to originally conclude it was not involved in biological signal processing related to information processing.

However, the absence of electroactivity in glia does not mean glia are totally inert. Recent years have shown glia to be amazingly active chemically, the most important of the activity currently known being calcium activity [VERK], [ARAQ]. Glia are known to possess active transporters that regulate concentration levels of extracellular chemicals, including glutamate, dopamine, and other important ligands used by neurons in cell-to-cell communication [ARAQ], [BERG]. One important recent discovery has been that glutamate uptake by glial cells stimulates a sharp rise in the glial cell's intracellular level of $[Ca^{2+}]$. It is thought that the mechanism for this is probably release of Ca^{2+} by the cell's endoplasmic reticulum via a metabotropic mechanism similar to the one we looked at earlier in the case of neuron cells. More important still, it is now known that glial cells can pass on ***calcium waves*** from glial cell to glial cell in the glial network [ARAQ], [VERK]. The precise mechanism by which this takes place is not yet fully understood, but the leading hypothesis is that this calcium transport takes place via the gap junction synapses connecting the glial cells. Calcium wave propagation is relatively slow – on the order of about 20 μm/s – but these waves can extend out to at least hundreds of microns from their source.

The rise of intercellular calcium concentration within the glial cell is known to be stimulated through glutamate uptake by the glial cell. There may be other mechanisms as well, but the glutamate uptake relationship is well established. Now, the mere fact that Ca^{2+} levels rise within a glial cell, and propagate from cell to cell, by itself implicates nothing more than that the internal chemical milieu of glial cells is responsive to neuronal signaling (since the excess Glu taken up by glia is due to neuronal signaling at glutaminergic synapses). In a manner of speaking, neurons "talk to" glial cells through their synaptic signaling activity. Were this all there is to it, it would be difficult to see any role for glial cells in biological signal processing.

But this is not all there is to it. It has been discovered that glial cells with elevated Ca^{2+} levels ***also release glutamate into the extracellular region*** [VERK], [ARAQ]. Again, the mechanism by which this takes place is not yet fully understood. The hypothesis with the most experimental support at this time is that glia release Glu via some mechanism probably similar to the neurotransmitter exocytosis process used by neurons. (It is the influx of Ca^{2+} through HVA calcium channels, and not the action potential, that actually releases neurotransmitter at the neuron's presynaptic terminal; the action potential merely opens the Ca^{2+} channels located in the terminal). Because glia heavily involve synapses in the cellular layout of brain cells, the release of Glu in the immediate vicinity of synapses could, in principle at least, have profound consequences for neuronal signaling.

The physiological evidence currently indicates the Glu exocytosis by glial cells[10] does not result in Glu entering into the tiny synaptic cleft separating the presynaptic terminal from the postsynaptic receptor site. Thus, glial Glu exocytosis does not *directly* excite synaptic responses. However, there is compelling evidence for the existence of Glu-binding receptors *outside* the synaptic area. These receptors, called ***extrasynaptic receptors***, include metabotropic Glu-binding receptors (MGluRs) and also appear to include NMDA receptors located on the presynaptic terminal itself [COCH], [GLIT].

The presence of NMDA receptors on the presynaptic terminal implies that Glu exocytosis by glial cells can ***modulate the amount of neurotransmitter release by the presynaptic terminal*** in response to an action potential. We will look at the mechanism for this in the next chapter, but the basic hypothesis is simple. If presynaptic NMDA receptors are enabled by glial Glu exocytosis, then there will be an additional influx of Ca^{2+} into the terminal in response to an action potential. The still-open question regarding this hypothesis is: Is the additional calcium influx significant compared to the influx due to the terminal's HVA calcium channels? If it is, then neuronal synaptic activity in one location could lead, through calcium wave propagation in the glial syncytium, to **modulation of the synaptic strength of other neurons** over a wide area. Existing evidence [GLIT], [COCH] seems to favor the hypothesis that this effect probably *is* significant.

The existence of extrasynaptic GluRs and MGluRs in the postsynaptic cell provide for at least the possibility that the glial syncytium might serve as a regional network for modulating the excitability of large numbers of local neuron groups in response to neuronal signaling by some members of the group. If in fact this signal processing mechanism exists, a proposition not yet established by physiology research, it has interesting potential consequences for network-level

[10] As we shall provisionally call it here, while awaiting additional clarification of the precise mechanism or mechanisms through future physiology research.

neuronal signal processing. For example, if it is the case that evocation and propagation of glial calcium waves has a threshold, then presumably one or more neurons would have to exhibit a somewhat higher level of firing activity, either individually or collectively, to produce it. Because calcium wave propagation is relatively slow, the glial syncytium might, in principle, be a mechanism for measuring the level of firing activity in a region and for causing enhancement (or suppression, depending on the precise mechanisms involved) of network-level responsiveness to network stimuli.

Not enough is known at present about the specifics of glial signaling to draw definitive conclusions about this speculation. However, the general question is interesting and potentially of significance because it is tied to mathematical questions involving necessary or sufficient conditions for promoting synchronized and oscillatory behaviors in neural networks. In recent years more and more neuroscientists have been drawn to the hypothesis that such behaviors by neural networks underlie cognitive processes, that network oscillations bias input selectivity, and facilitate synaptic plasticity (the putative physiological mechanism for learning and memory) [BUZS], [VARE]. Consequently, there has been considerable work by mathematicians striving to understand what requirements on signal coupling, network interconnects, global vs. local signal connectivity, and relative signaling delay properties promote different kinds of synchronicity and oscillatory behaviors in model networks [CAMP1], [MEDV], [WANG]. To date the models used in these studies have attempted to remain at least somewhat faithful to known properties of neural networks but have not considered how or if the picture may change if there is a signaling syncytium capable of **globally and non-specifically biasing** these factors in a network. This is an important question for neural network research because it is known, through the work of Grossberg in the 1970s, that non-specific signaling within complex neural network systems is crucial for the possibility of a number of important factors in neural network dynamics. This is especially the case in adaptive resonance theory (ART) [GROSS5-6, 11-12, 19-20].

Finally, some researches have speculated that glial cells might play a more direct role in synaptic plasticity mechanisms. Long-lasting changes in synaptic weight coupling, known as long term potentiation (LTP) and long term depression (LTD), are extremely important in neuroscience because these are thought to underlie and provide the biological substratum for learning and memory phenomenon. The question of whether or not glial cells participate in the plasticity phenomena is presently not even remotely close to being settled and is, as a matter of fact, a topic of somewhat heated controversy at present.

No general modeling schema, comparable to the unified treatment of neurons provided by the Hodgkin-Huxley schema, has been proposed to date for the glial syncytium. Because glia are not

electrically active *in vivo*, but because they appear to be chemically active in their reciprocal signaling with neurons, a schema such as the Linvill schema presented in this chapter appears to be an attractive first step in the *quantitative* modeling of the glia factor in biological signal processing. There is, however, a great deal of physiological research still needed to enhance and quantify the various elements in the Linvill schema before we can achieve more than a first-order approximate model of the global effects of calcium-wave signaling. It is a fertile topical area for fresh neuroscience research.

§ 6. The Reactance Element in the Linvill Modeling Schema

In section 2.3 of this chapter the Linvill modeling schema was introduced. Of the five Linvill network elements introduced, only the mathematical description of the first four was discussed. Treatment of the reactance element was postponed for later. The time for that treatment has now arrived.

We have seen that metabotropic signaling plays an important control function in biological signal processing. Metabotropic signaling occurs by means of cascade biochemical reactions in the cell that alter basic properties in the flow of ionotropic signaling pathways. The reactance element is the element in the Linvill network modeling schema that models chemical reactions.

The basic element shown in figure 4.3 has two inputs and one output. The reactance can be easily extended to take into account more input reactants and/or to produce more than one reaction product. In this section the action of the reactance element is illustrated for the simplest case of two inputs and one output as shown in figure 4.13 below.

Consider the case of a simple reaction such as

$$2H_2 + O_2 \rightarrow 2H_2O$$

or, more generally in terms of concentrations of substances,

$$2\nu_1 + \nu_2 \rightarrow 2\nu_3 .$$

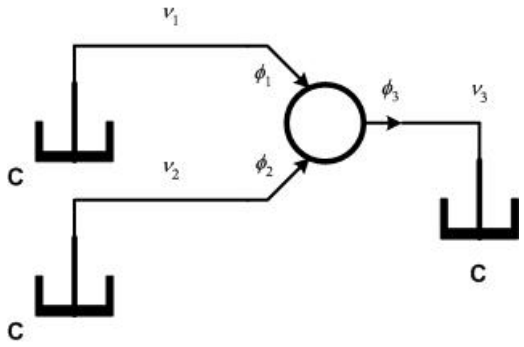

Figure 4.13: Linvill reactance element example.

We assume all three substances are co-located within the same volume within the cell. Because the substances represent different chemical species, three storance elements are required, as shown in the figure. Noting the flux directions indicated in the figure and applying the storance element law, we have

$$\phi_1 = -C\dot{v}_1; \quad \phi_2 = -C\dot{v}_2; \quad \phi_3 = C\dot{v}_3.$$

Noting the stoichiometric coefficients in the chemical reaction equation above, we also have

$$\phi_1 = \phi_3; \quad \phi_2 = 0.5 \cdot \phi_1.$$

Chemical reaction kinetics are governed by what is known as the mole balance equation [FOGL: 6-16] and by the form of the reaction rate equation. In general, reaction rate equations are algebraic equations, rather than differential equations, and are frequently deduced from experimental data. Generally, a reaction rate equation would be of the form $\phi_i = f_i(v_1, v_2, v_3)$ where f_i is some algebraic function of the concentrations of the three substances involved in the reaction [FOGL: 73-113]. For purposes of our present example, we will assume the reaction is governed by the simplest form of reaction rate expression, namely the second order reaction,

$$\begin{aligned} C\dot{v}_1 &= -\alpha \cdot v_1 \cdot v_2 \\ C\dot{v}_2 &= -0.5 \cdot \alpha \cdot v_1 \cdot v_2 \\ C\dot{v}_3 &= \alpha \cdot v_1 \cdot v_2 \end{aligned} \quad .$$

Here α is a non-negative proportionality constant for the reaction rate. Note that the simple second order reaction model used here makes the system of differential equations describing the network a nonlinear system model even if all the other Linvill elements in the network are described by linear differential equations.

In a more complex network than the one depicted in figure 4.13, the first two equations above merely enter in as terms in the differential equation for nodes 1 and 2, respectively and account for the disappearance of substances v_1 and v_2 that occurs during the chemical reaction. The third differential equation above is a new term introduced into the overall set of network equations by the reactance element. In other words, a reactance element having only a single output product introduces one new differential equation into the system model, namely that of the reaction product. In general, one new differential equation is introduced for each output product. The relative amounts of flux associated with each substance is determined from the stoichiometry of the chemical reaction [FOGL: 33-35].

In some important biochemical reactions one of the reactants, say v_2 for example, may merely act as a catalyst and take no other part in the reaction. The simplest example would be the case where v_1 is an inactive isomer and v_3 is an active isomer form of the same substance. In this case

we would have $\phi_2 = 0$ because catalyst ν_2 is neither increased nor decreased by the reaction it catalyzes. Often the reaction rate in such a case might involve a first-order reaction, $f = \alpha \cdot \nu_2$, in the expressions for ϕ_1 and ϕ_3. In such simple cases as this, the Linvill network can often be simplified by the introduction of a sixth element, called a **reactor**, which is mathematically identical to the transporter element in figure 4.3 except that the substances represented at the two terminals are different substances. Examples of the use of a reactor element are discussed in chapter 5. The reactor element can be regarded as a special case of a one-input/one-output reactance.

At the present time, it is the unfortunate case that the research literature reporting the findings of biochemical studies in neuroscience frequently omit findings regarding the specific reaction rate kinetics of the biochemical reactions being studied. In the opinion of your author, this is largely due to the fact that computational neuroscientists have not yet carried out much work on the mathematical modeling of metabotropic processes and, as a consequence, have posed no research questions to the biochemical community to help direct specific research investigations. It can be hoped that the introduction of the Linvill modeling schema may help to correct this situation. In the absence of reported experimental facts, the mathematical modeler can only have recourse to phenomenological guesses of what form of reaction rate equation f might be involved in a particular system under study. Quantitative results from such modeling work can serve to pose questions to other researchers that subsequent experiments can confirm or refute. One example of this is a recent work by Ramirez, Wells, and Lew on the modeling of monoclonal antibodies in the treatment of methamphetamine addiction [RAMI].

Exercises

1. Using either MATHCAD® or a computer program of your own design, plot the Boltzmann equation ($g_{max} = 1$) over the range from -100 mV $< V_m <$ 100 mV for V_{50} values of –70, –50, and –30 mV and with k values of –5, + 5, and +20 mV.
2. Prove the two models in Figure 4.1 are equivalent if G in the Thévenin equivalent is equal to the sum of $G_1 + G_2$ and the battery potentials in both circuits are the same.
3. Using equations (4.4), plot the steady-state m_{Ca} over the range from -100 mV $< V_m <$ 100 mV.
4. Using the numerical values given in the text and either MATHCAD® or a computer program of your own design, reproduce Figures 4.2.
5. Huguenard and McCormick express the activation and inactivation constants for their LVA calcium channel model using a Boltzmann function for m_∞ and h_∞. For the activation constant they use $V_{50} = -57$ mV and $k = 6.2$ mV with $j = 2$. For the inactivation constant they use $V_{50} = -81$ mV and $k = -4.0$ mV. Their time constant expressions are

$$\tau_m = \frac{1}{\exp\left(-\left(V_m + 132\right)/16.7\right) + \exp\left(\left(V_m + 16.8\right)/18.2\right)} + 0.612$$

$$\tau_h = \begin{cases} \exp\left(\left(V_m + 476\right)/66.6\right), & V_m < -80 \text{ mV} \\ \exp\left(-\left(V_m + 22\right)/10.5\right) + 28, & V_m \geq -80 \text{ mV} \end{cases}$$

Plot the activation and inactivation curves for this channel.

6. Convert equation (4.9) to a difference equation.
7. Derive the difference equations for equation (4.10) as shown in the text.
8. Plot the activation constants, equations (4.19), using the same calcium concentrations as used in plotting figure 4.8.
9. Plot the activation and inactivation constants for the Huguenard/McCormick A_1 and A_2 channel parameters given in Table 4.1.
10. Propose a generic circuit model for a two-compartment neuron model in which the first compartment represents the cell soma and dendrites and the second compartment represents the axon. Draw a schematic diagram of your proposed two-compartment model schema.
11. Plot the activation and time constant curves for the h-current using the parameter values given in the text.
12. Find the difference equation description for the NMDA channel.
13. Plot the NMDA channel conductance for membrane potentials of –65, –60, and –55 mV.